A Proposed Spacecraft Design to Track and Map Plastic Debris in Pacific Ocean

*Preliminary design developed by Group 3

1st Aníbal Guerrero Hernández
03771704
Technical University of Munich (TUM)

2nd Leonie Büssenschütt
03768216
Technical University of Munich (TUM)

3rd Anna Kurzmann
03711498
Technical University of Munich (TUM)

5th Falk Ramin
03780703
Technical University of Munich (TUM)

7th Rakesh Vaskar
03766075
Technical University of Munich (TUM)

6th Danica Rayen
03768111
Technical University of Munich (TUM)

4th Ditsa Mukherjee
03766342
Technical University of Munich (TUM)

I. Introduction - Anibal

The exploration of space has captivated the human imagination for generations, inspiring pioneering endeavors to reach beyond the confines of our planet. As we venture deeper into human knowledge, the development of spacecraft plays a pivotal role in unlocking the mysteries of the universe and advancing our understanding of our environment. The quest for knowledge and the pursuit of scientific discoveries have fueled the evolution of spacecraft design, leading to cutting-edge technologies and innovative engineering solutions.

This report delves into the intricate process of spacecraft design. From its conceptualization to the realization of a fully functional spacecraft and how subsystems dynamically change and shape each other, finding optimal solutions through compromise.

Spacecraft design is a multidisciplinary endeavor that brings together aerospace engineering, astrophysics, materials science, computer science, thermodynamics, and various other fields. It involves a delicate balance of intricate technicalities, where every component's performance and interaction are critically evaluated to ensure operation and mission success. Challenges such as limited resources, harsh space conditions, and the quest for optimal performance drive to push for innovation.

This report aims to provide a comprehensive understanding of the key phases in spacecraft design, starting from defining the mission objectives and requirements, through the selection of propulsion systems, payload configurations, power management, thermal control, and attitude determination and control. Additionally, we explore the methodologies employed to evaluate trade-offs and make informed decisions, ensuring that the spacecraft's design aligns perfectly with the mission's unique goals and constraints.

Furthermore, the report will delve into the role of software tools, such as MATLAB scripts, that facilitate dynamic calculations, GMAT system simulations, and contacting providers to obtain information about COTS subsystems and services they offer, streamlining the design process and enhancing overall efficiency.

II. Work Logic, Methodology, Approach, Processes - Anibal

The proposed spacecraft design is developed by conducting a thorough mission analysis. Mission objectives are developed and requirements for each subsystem are determined. Iterations between payload and orbit selection are fundamental to designing the other subsystems. Once the payload selection is frozen, a full orbital analysis is performed and the other subsystems such as thermal, power, propulsion, and ADCS, start iterating through designs and parameter selections. As the project advances these subsystems freeze their design and launch sites, and ground stations are selected. Additionally, a physical model of the spacecraft is developed, and compatibility between subsystems is checked through a final iteration.

III. Tools - Anibal

A. GMAT - Anibal

GMAT (General Mission Analysis Tool) serves several purposes. First, it serves as a visualization and validation tool in orbit selection and determination performed through MATLAB. Second, it is employed to analyze and optimize station-keeping manoeuvres for a satellite operating at the proposed orbital altitude. The simulation focuses on assessing the effects of aerodynamic drag on the satellite and how that incurs orbit degradation. With GMAT, the precise time required for the satellite's orbit to degrade by *30km* is determined. subsection XIII-E contains a visualization of the orbit

degrading and the time were station-keeping maneuvers have to be performed.

B. MATLAB

In the development of the spacecraft's design, a suite of MATLAB scripts has been developed to perform dynamic calculations and assess how systems interact with each other. Scripts are divided into functions, as followed in Object-Oriented Programming (OOP), and is best practice to maintain the code readable, accessible, and transferable. Each function is responsible for a specific task. Additionally, necessary comments are included in the scripts so parameters and relevant explanations are provided. These scripts enable a comprehensive evaluation of the propulsion system, the attitude determination and control system, orbit determination and payload selection, as well as sizing solar arrays, batteries and achieving thermal control. These will ensure that the mission requirements are met. A representation of all functions categorized into their relevant categories is shown in Figure 1.

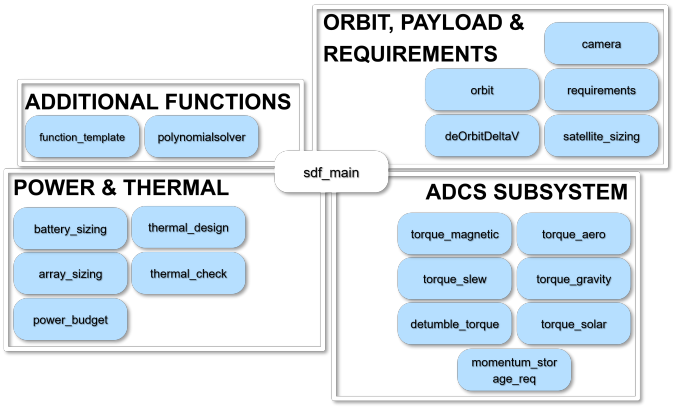

Fig. 1. MATLAB scripts

In total, more than *20* functions and *1000* lines of code have been implemented in the programming resolution of the project's objectives to determine optimized parameters.

- Main Script: *sdf_main.m*, serves as the entry point for the spacecraft design process. It calls and coordinates the execution of various functions and scripts to ensure a systematic analysis of critical aspects of the design.

Other functions are contemplated in Appendix XXX, please consult for further details.

Main contributors towards the MATLAB script development:

- Anibal - General script development of most of the project. All subsystems.
- Anna - Power and thermal subsystem related functions.
- Falk - ADCS related functions.
- Leonie - Orbit and payload related functions.

C. STELA - Anna

STELA is an open-source de-orbit calculation software developed by the french space agency CNES. It uses the drag area of the satellite, orbital parameters and different environmental perturbations like atmospheric drag or moon gravity as input to calculate the de-orbit time of a satellite. The advantages of STELA are, that it has an included Area Tool in which the rough geometry of the satellite can be built and the drag area can be calculated. It has the option for the assumption of random tumbling, fixed rotation axis or fixed flight direction. The second advantage is its fast computation time which is below one minute for a de-orbit analysis over 50 years with an ephemeris step of 24h.

IV. Mission Objectives - All

Based on the given mission statement the mission objects were developed. They have been summarized into the following primary and secondary mission objectives [1]:

Primary Mission Objectives

1) To identify, track and map the location and size of plastic clusters in the Pacific Ocean with optical instruments.
2) To store and analyze the data to compare it with previous measurements.

Secondary Mission Objectives

1) To visualize the data to raise awareness of plastic pollution.
2) To predict the patch movements using mission data.

V. Requirements - All

The requirements for the mission have been grouped in the categories functional, operational, constraints and subsystems [1]. Each requirement has been derived based on the given project description, additional knowledge and norms. The requirements are listed in Table XXVIII.

VI. Payload - Leonie

One of the first subsystems to consider while designing the spacecraft was the payload. The payload for the given mission consists of an optic and a sensor. One can select these components individually from one another or select a pre-existing combined system. Since the already combined systems are usually well tested and cheaper compared to the custom made components, the selection focused primarily on the pre-integrated systems. In case that no suitable choices can be found, one could always go back to the more basic approach.

A. Selection Criteria - Leonie

To start with the selection of already existing systems, selection parameters were defined based on the requirements shown in the Table XXVIII. The GSD as well as the wavelengths were given by the requirements [1-001], [4-101], [4-002]. Another important aspect that was considered was the Swath length. This was calculated in an iterative process with the orbital determination by using the following formula:

$$\frac{2\pi r_E}{2N_O} = \frac{2\pi \cdot 6378\ km}{2 \cdot 160} = 125.2\ km \tag{1}$$

Where r_E is earth radius, and N_O is the number of orbits until the repetition point. To determine N_O, a low earth orbit (LEO) was assumed. N_O was obtained due to the revisiting requirement of every 10 days and the orbital period of similar satellites being roughly 90 minutes in low earth orbits and thus leading to approximately 16 rotations per day. A few cameras were selected and compared to the selection parameters with them being the **swath length of 125 km, a GSD of 36 m and the wavelength requirements of 442 nm and 884 nm**.

B. Camera choices and Selection - Leonie

The selected cameras are shown in Table I. HyperScape100 has a lot of benefits, but the field of view was too narrow and thus the swath length too small. JG-P1100G-Push Broom seemed appropriate, but it is not fully developed yet and not all necessary information is specified. WorldView–110 had the same problem as with HyperScpae100. The field of view was too narrow and the camera in general too large and "powerful" for the means. HyperScape50 came already very close to the selection criteria. GSD, wavelength and swath width are similar to the requirements. In addition, the size is suitable for a cubesat and the weight is very low. HRVI-6HD 2nd Generation could also be an option at first sight. Its swath width is smaller than the swath width of camera 4, but for a much smaller GSD. Therefore, the altitude of the satellite we could be increased and thus the swath width as well. The problem with the camera is that it cannot reach the 442nm wavelength requirement and the size of the HRVI-6HD 2nd Generation is much larger than the size of HyperScape50. That is why **HyperScape50** was selected since it meets all given selection criteria. Additionally, the size and mass of the camera are feasible for a cubesat. The scanning technique of this camera is push broom which provides a "uniform response function in the along-track direction" which is beneficial for the mission [1]. The main camera characteristics of the considered cameras are summarized in Table I. A picture of the HyperScape50 can be seen in Figure 2.

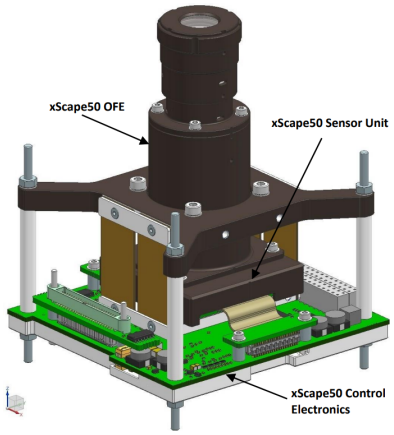

Fig. 2. HyperScape50 [7]

To verify the suitability of the HyperScape50 camera, the feasibility of the focal size was checked. This can be done by

TABLE I
CAMERA SPECIFICATIONS

Camera Name	**Hyper-Scape-100** [3]	**JG-P1100G-Push Broom** [6]	**WorldView –110 (WV110)** [4]	**Hyper-Scape-50** [5]	**HRVI-6HD 2nd Gen.** [2]
GSD [m]	4.75	2.5PAN 10 MS	1.8	29.3m	4.6
Wave-length Range [mm]	442 - 884	400 – 520 770-895	400 – 650 770-895	442 – 884	450 – 900
Aperture [mm]	95	-	1100	11.75	89
Focal length [mm]	580	-	13300	93.99	500
Swath width [km]	19.4	-	16.4	120	70
Orbital height [km]	500	-	694	500	500
Mass [kg]	1.1	6.2	-	0.44	-
Size	1.5U	-	3m max	1U	29U

using the following equation which gives a rough estimation for the focal size [1].

$$f = \frac{ps \cdot h}{GSD} = \frac{5.5 \cdot 10^{-6}\ m \cdot 6 \cdot 10^{5}\ m}{36\ m} = 0.0917\ m \quad (2)$$

Here ps is the pixel size and h is an assumed value for LEO. Since the calculated focal size is smaller than the focal size of the selected camera, it is a feasible choice.

C. Data rate - Leonie

In order to size the TT&C subsystem, the data rate of the selected camera needed to be calculated. The data rate DR of the HyperScape50 was determined by the Equation 3 which holds for small swath lengths. It is determined by multiplying the pixels in cross-track and along-track direction by the desired pixel size [1].

$$DR = N_p \cdot \frac{v_{sso}}{GSD} \cdot B_p \quad (3)$$
$$= 4096 \cdot \frac{7566\ \frac{m}{s}}{36} \cdot 12\ bit = 10.33\ Mbps$$

N_p here is the number of pixel of the camera cross-track, v_{sso} is the velocity of the spacecraft see section VII and B_p is the number of bits per pixel required [1].The required wavelengths lie in the visible and near infrared spectrum. To visualize the data, 12 bits shall be used for a colour image. The data rate can be reduced by compressing the data prior to transmitting. The HyperScape50 also comes with an internal storage of 128 Gigabyte [5] so that in case of no upstream connection the data can be saved for up to $\frac{128 \cdot 10^3 \cdot 8\ Mbit}{10.33\ Mbps} = 27.7$ hours.

VII. Orbit Selection - Anibal & Leonie

A. Initial thoughts - Leonie

The orbit for our spacecraft shall fulfill the given requirements. One of them is the coverage of the entire Pacific Ocean within ten days. To get a starting point for the orbit, research was conducted on the orbits of similar missions. Many of the current Earth observation satellites are in a low Sun-Synchronous Orbit (SSO). These orbits can be adjusted to become frozen orbits such that they repeat after a specified amount of time. By that, the same place can be repeatedly visited under similar light conditions. This increases the image quality and comparability. In addition, they can have a low to no eclipse time which would require only a small battery and thus less weight [8]. Highly elliptical orbits were considered since this orbit type could be adjusted to fly above the Pacific Ocean only and could decrease the repetition time. However, this type of orbit would lead to high velocities and altitudes for our spacecraft. The payload selection for such an orbit would be very difficult. A high-resolution camera would be needed. Hence, the repeating SSO was chosen as the spacecraft's orbit.

B. First approximation - Leonie

The orbital height for a SSO usually ranges between 600 – 800 km [9]. The determination of the orbit strongly depends on the camera and sensor that was selected. The approximation of swath width, the GSD, and wavelength requirements helped to select a potential camera and sensor for the spacecraft see section VI. With the given values of the camera HyperScape50, the maximum swath length was calculated $l_{swathmax}$ achievable by the camera via:

$$l_{swathmax} = res \cdot GSD = 4096 \cdot 36 \ m = 147.5 \ km \quad (4)$$

With res being the resolution of the camera and GSD being the required ground sampling distance. This result was obtained to calculate the orbital height h_{opt} for the maximum swath length.

$$h_{opt} = \frac{l_{swathmax}}{tan(FOV)} = \frac{147.5 \ km}{tan(13.68\,\mathrm{deg})} = 605.8 \ km \quad (5)$$

Where FOV is the field of view of the selected camera. With the formula for the repeating ground tracks the number of orbits until the repetition point was determined and cross-checked with the repetition requirement of 10 days [8].

$$N_O = \frac{k_{days2rep}}{(\frac{h_{opt}+r_e}{42164.17})^{\frac{3}{2}}} \approx 143 \quad (6)$$

After rounding up the value to an integer the final orbital height could be calculated. This was done by rearranging Equation 6 to h_{opt} and thus getting:

$$h_{opt} = 42164.17 \cdot (\frac{k_{days2rep}}{N_O})^{\frac{2}{3}} - r_e = 585.2 \ km \quad (7)$$

The orbital height is slightly lower than the first approximation of 605.8 km. This is due to the fact that N_O needs to be an integer in order to lead to a repeating sun-synchronous orbit. It is a conservative approach to choose a lower value for the final orbital height than the first approximation since the first calculation was based on the maximum swath possible. Now there is still some margin left in case the outer pixels of the camera scan do not have a good enough resolution.

C. Solar Synchronous Orbits - Anibal

Earth's equatorial radius is greater than its polar radius due to its equatorial bulge and spin. The torques exerted by this extra equatorial mass cause nodal regression of a satellite orbit, analogous to a spinning top that wobbles due to gravity [10], [11]. Figure 3 demonstrates the difference between a polar orbit and a solar synchronous orbit. The polar orbit is observed in Figure 3(A). It is a case where the orbit is fixed in the inertial frame due to zero regression. In this case, although the local sidereal time remains the same throughout the year, the local solar time varies according to Earth's position relative to the Sun. However, if uniform solar illumination is to be provided for satellite imaging, the nodal regression should match Earth's yearly revolution rate around the Sun. This occurs in solar synchronous orbits and is one of the main advantages of using SSOs. Uniform solar illumination leads to a reduction in battery capacity, which incurs a reduction in battery size and improved scanning resolution.

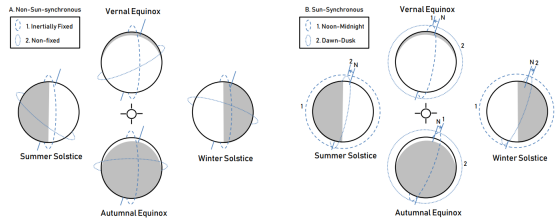

Fig. 3. Satellite orbits that are not Solar-synchronous (A) and Solar-synchronous (B). [12]

The spacecraft orbit's regression rate in SSOs is given in Equation 8, which is $360/365.2422 days = 0.9856/day = 2 \times 10^{-7} rad/s$. $\dot{\Omega}$ is the time derivative of longitude of ascending node Ω and is a function of the semi-major axis (a), eccentricity (e), and inclination (i). Other parameters include R_E as Earth's equatorial radius, $J_2 = 1.08263 \times 10^{-3}$ as Earth's oblateness coefficient, and $\mu_E = 3.986 \times 10^5 km^3 s^{-2}$ as Earth's standard gravitational parameter. Figure 4 depicts the influence of the semi-major axis with the inclination of Solar-synchronous orbits and their regression rate.

$$\dot{\Omega} = -\frac{3R_E^2 J_2 \sqrt{\mu_E}}{2a^{7/2}(1-e^2)^2} cos(i) \quad (8)$$

As mentioned in subsection VII-A and subsection VII-B, the orbit has repeating ground tracks (RGTs). This happens if a satellite's ground track exactly repeats its pattern after a certain number of days, $k_days2rep \equiv N_D$. With an Earth nodal period T_N and a spacecraft orbital period T_s, the satellite completes N_O revolutions around Earth after N_D nodal days [12].

$$N_S T_S = T_N N_D \quad (9)$$

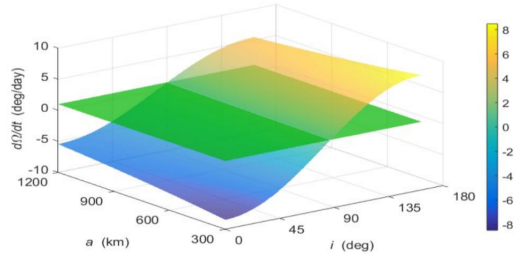

Fig. 4. Effect of semimajor axis and inclination on the orbital nodal regression rate with zero eccentricity. The line intersection defines circular SSOs.

Substituting T_N and T_S, Equation 10 is developed. The spacecraft's angular velocity, n, is equal to:

$$\frac{2\pi}{T_S} = \left(\frac{\mu_E}{a^3}\right)^{1/2} \tag{10}$$

This angular velocity is changed by Δn in the numerator of Equation 11 due to Earth's oblateness, which is shown in Equation 12 [12]. The argument of perigee is also perturbed according to Equation 13 [12]. Lastly, it is worth remembering Earth's spin rate, $\omega_E = 360/1day = 7.29 \times 10^{-5} rad/s$.

$$\tau = \frac{N_S}{N_D} = \frac{T_N}{T_S} = \frac{2\pi/(\omega_E - \dot{\Omega})}{2\pi/(\dot{M} + \dot{\omega})} = \frac{n + \Delta n + \dot{\omega}}{\omega_E - \dot{\Omega}} \tag{11}$$

$$\Delta n = \frac{3R_E^2 J_2 \sqrt{\mu_E}}{4a^{7/2}(1-e^2)^2}(2 - 3sin^2 i) \tag{12}$$

$$\dot{\omega} = \frac{3R_E^2 J_2 \sqrt{\mu_E}}{4a^{7/2}(1-e^2)^2}(4 - 5sin^2 i) \tag{13}$$

Setting $\dot{\Omega} = \omega_E S = 0.9856/day$ and $J_3 = -2.5327 \times 10^{-6}$ and calculating the eccentricity with Equation 14:

$$e = -\frac{1}{2}\frac{J3}{J2} sin(i) \tag{14}$$

Equation 15 encapsulates the influence of the orbital altitude on the inclination and other orbital elements.

$$\sqrt{\frac{\mu_E}{(R_E+h)^3}} + \frac{J_2 R_E^2 \sqrt{\mu_E}}{(R_E+h)^{7/2}} * \left(\frac{8}{3}\frac{(R_E+h)^7 \omega_E S^2}{J_2^2 R_E^4 \mu_E} + \frac{3}{2}\right)$$
$$+(\omega_E - \omega_E S)\tau = 0 \tag{15}$$

This relationship is reflected in Figure 5. As can be observed, there are discrete solutions of the equation corresponding to different combinations of orbital altitude, inclination, and days until repetition.

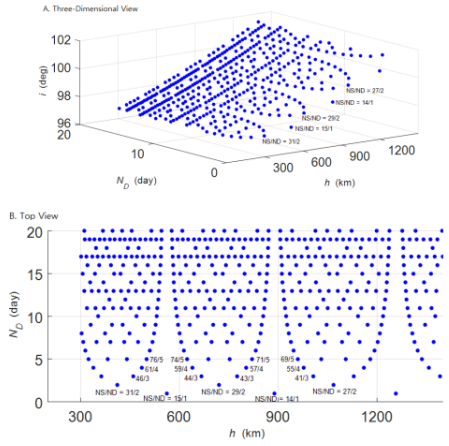

Fig. 5. SSORGT orbit altitude and inclination in (A) 3-dimensional view and (B) top view. [12]

D. Orbital Elements - Anibal

The remaining orbital elements are the *Right Ascension of the Ascending Node (RAAN)* (Ω), the *argument of periapsis* (ω), and the *true anomaly* (ν).

The *RAAN* is used to align the spacecraft's orbital plane with the vernal equinox. Therefore, it corresponds to the longitude of maximum sun exposure (midday). In this case, the longitude corresponding to the middle of the ocean is 124.30.

The *argument of periapsis* is set to 270. It defines the point of closest approach to Earth. As the eccentricity is almost negligible, the argument of periapsis has been set analogous to other Earth observation missions, as velocity and altitude will not vary significantly between different points throughout the orbit.

Finally, the *true anomaly* is set to 360, equivalent to 0. This is the spacecraft's reference point and corresponds to the periapsis. Thus, the point in which the repeating ground track will repeat itself.

In Table II, all orbital elements have been listed. Additionally, an extra column has been added to demonstrate which orbital element addresses certain requirements.

TABLE II
ORBITAL ELEMENTS

Orbital Element	Value	Requirements
Eccentricity, e [-]	0.00296	**[3-004]**
Semimajor Axis, a [km]	6963.39	
Inclination, i []	97.7296	**[2-005]**
RAAN, Ω	124.30	
Argument of Periapsis, ω	270	
True Anomaly, ν	360	

VIII. THERMAL AND POWER SUBSYSTEM - ANNA

A. Power Budget - Anna

The power budget of the spacecraft can be derived as sum of the power requirement of each is subsystem and can be split into two cases: operational mode in sunlight and survival mode during the eclipse. The values are listed in Table III:

TABLE III
POWER BUDGET

Subsystem	$P_{Sun}[W]$	$P_{Eclipse}[W]$
Camera [7]	7.4	n.a.
Telecom [13]	22.5	11
Attitude Control [14]	1.71	1.71
Solar Array Drive Assembly [15]	0.5	0.001
Power Control Unit [16]	1.25	1.25
Computer Subsystem	2	2
Heater	0	9
Propulsion System [17]	10	10
Total Power	**54.43**	**41.95**

A margin of 20% in this early design stage is used to calculate the total power requirement. The camera can only operate during sun-phase since the used wavelengths are part of the visible spectrum which means no images can be taken at night. For the telecommunication it is assumed that during eclipse only the receiver (6W) and the electronics necessary for modulation (5W) are in operation. No data is transmitted during eclipse so the power requirement of 11.5W of the transmitter is not needed in eclipse mode. The solar array drive assembly is in idle mode during eclipse because the solar arrays are not receiving any sun and must not be rotated. The heater is located near the ADCS and battery due to the critical operational temperatures and is only active during eclipse to maintain the required temperature. All other subsystems including attitude control, power control unit, computer subsystem and propulsion are active in both phases.

B. Trade Off and Requirements - Anna

Considering the low power requirement, the orbit near the earth and the mission duration of 5 Years, Solar Cells and rechargeable batteries are chosen as Subsystems. Solar Cells fit for low power requirement and are cheaper and not hazardous in comparison to radioisotopes [1]. For the batteries a Li-Ion Cell is chosen, since they are the state of the art for a high energy density, rechargeable and flight proven [18]. The requirements of the thermal and power subsystem can be found in the Appendix in Table XXVIII from [4-301] to [4-303] for the solar arrays (including power and size) and from [4-401] to [4-403] for the battery (including capacity, life cycles and material).

C. Battery - Anna

The required battery capacity can be calculated according to Equation 16 by using the required power during eclipse $P_{Eclipse}$, eclipse duration $t_{Eclipse}$ and the depth of discharge (DOD) of the battery.

$$C_{bat} = \frac{P_{Eclipse} \cdot t_{Eclipse}}{60 \cdot 60} \cdot \frac{100}{DOD} = 62.2 \ Wh \qquad (16)$$

The selected battery shall have at least the calculated battery capacity, shall be Li-Ion and shall survive 5 Years in LEO orbit which corresponds to 27000 cycles (Appendix: Table XXVIII). Table IV shows possible batteries for the mission: 4SIP VES16, UHP341440 NCA and NanoPower BP4 are not fulfilling the power requirements, HE602030 NCA does not meet the necessary cycle number and 43Ah Space Cell has much more power than necessary and would have increased volume and mass. According to these requirements from Table XXVIII, the 30Ah Space Cell Battery from the company Eaglepicher is selected and the DOD of 40% is used for the calculations.

TABLE IV
BATTERY TRADEOFF

Battery	**Power [Wh]**	**DOD [%]**	**Cycles**	**Material**
4SIP VES16 [19]	64	30	25 000	Li-Ion
30 Ah Space Cell [20]	133.95	40	40 000	Li-Ion
43Ah Space Cell [21]	194.31	40	40 000	Li-Ion
UHP341440 NCA [22]	27	80	2 000	Li-Ion
HE602030 NCA [23]	198	80	2 000	Li-Ion
NanoPower BP4 [24]	43	20	60 000	Li-Ion

D. Solar Arrays - Anna

The required solar array power can be calculated with Equation 17 by using the power requirements during sun-phase and eclipse and the efficiency of the battery.

$$P_{Array} = (P_{Sun} + \frac{P_{Eclipse}}{\eta_{battery}}) \cdot (1 - L_{Deg})^t = 116 \ W \qquad (17)$$

The efficiency of the battery is assumed to be 32 % [25], the efficiency of the solar arrays 90 %[18] and the degradation of the solar arrays with 2.75% per year [1]. The size of the solar array is obtained by Equation 18 and using the Heat Flux of the sun ϕ_{sun}, the array efficiency η_{array}, the viewing factor F and the angle between the normal of the solar array and the sun θ.

$$A_{Array} = \frac{P_{Array}}{\phi_{sun} \cdot \eta_{array} \cdot F \cdot cos(\theta)} = 0.31 \ m^2 \qquad (18)$$

According to the power requirement, two wings Hawk 27AS118 from MMA Design are selected from the options depicted in Table V. It fulfills the power requirements and has the feature, that each wing is stored within 3Ux2U and deploys to 4 panels each 200x300mm. Additionally, a solar array drive mechanism is available by Honeybee Robotics in cooperation with MMA Design, that ensures that the panels are always perpendicular to the sun and has a small volume of 100x100x6.5mm [15].

TABLE V
SOLAR ARRAY TRADE OFF

Company	Power [W]	Size [mm]	Feature
ISISSpace [26]	17	6U	n.a.
Sparkwing [27]	88 to 360	up to 800x1230	n.a.
Spacetech [28]	up to 5kW	not given	n.a.
Endurosat [29]	17W	6U	deployable
MMA Design Hawk 27AS118 [30]	118	2 Wings 4x200x300	deployable rotateable

E. Power Control Unit - Anna

A power control unit is necessary, to control the power flow from the solar arrays to the payload, subsystems and the battery. Therefore, the NanoPower P80 from GOMSPACE is selected, since it is flight proven, weights only 368g and can handle solar power generation of up to 300W [16].

F. Thermal Control - Anna

Thermal control elements are necessary, since the satellite experiences high variations in temperature between sun phase and eclipse. Table VI shows the survival and operational temperatures of each subsystem, that shall not be exceeded.

TABLE VI
SURVIVAL AND OPERATIONAL TEMPERATURES SUBSYSTEMS

Subsystem	$T_{Operation}$ [K]	$T_{Survival}$ [K]
Electronics [16]	358 233	358 233
Battery [20]	333 253	333 233
ADCS [14]	333 263	343 253
Solar Array [1]	383 123	403 73
Payload [7]	323 263	333 253
TT&C [13]	358 228	358 228

A coating shall be used as a passive thermal control element. A heater near the payload and ADCS system is used as an active thermal control element. Table VII shows the available coatings and their main properties.
The coating shall provide sufficient temperatures in the hot case: Beta cloth aluminized, black colour and metallic aluminum are not suited, because they exceed the temperature requirements. The remaining coatings have similar cold case temperatures of around 245K (except vacuum deposited aluminum) but different hot case temperatures, which all fulfill the requirements. Vacuum deposited aluminum would additionally fulfill the cold case requirements but the manufacturing process is complicated and expensive. Therefore, Mylar MLI is chosen because it is cheap, flight proven and available on the market. The temperature in the cold case is still to cold for the ADCS and payload to survive. In further simulations there shall be two additionally points taken into account that have been neglected in this first approximation: First, the equilibrium temperatures may not be reached due to the fast change between sun phase and eclipse. A dynamic simulation shall be done for that instead of a static equilibrium. Second, the temperature distribution in the satellite varies depending on the distances to the outer shell or to the heater for example. By taking the correct distribution into account, the operational and survival temperatures of each component may not be exceeded. As soon as the distribution is known, heat pipes could be installed to cool for example the battery and heat the ADCS.

TABLE VII
COATINGS TRADE OFF

Name	α	ϵ	T_{sun} [K]	$T_{eclipse}$ [K]
Beta Cloth [31]	0.45	0.8	307	246
Beta Cloth Aluminized [31]	0.37	0.3	364	281
Tedlar Reinforced [31]	0.3	0.8	289	246
Kapton [31]	0.41	0.81	302	245
Teflon Baked [31]	0.1	0.85	256	244
Teflon Coated [31]	0.14	0.75	268	248
White Colour [32]	0.12	0.929	257	242
Black Colour [32]	0.86	0.95	332	242
Metallic Aluminum [32]	0.08	0.04	458	427
Vacuum Deposited Aluminum [18]	0.1	0.25	313	290
Mylar MLI [32]	0.24 BOL 0.5 EOL	0.78	314	246

IX. ATTITUDE DETERMINATION AND CONTROL SYSTEM - FALK

The Attitude Determination and Control System (ADCS) controls the orientation and attitude of a satellite in space. It is equipped with actuators and sensors to achieve and maintain a desired attitude. The design drivers for the ADCS were based on several requirements that had to be attained see Table XXVIII. Various types of spacecraft control methods exist which can be distinguished by passive techniques like Gravity-gradient or Spin stabilization, and active methods like 3-axis control. For this mission, a 3-axis control system was chosen due to the high accuracy and maneuverability requirements, despite being more complex and expensive than passive methods. The design process of the ADCS involved defining the different disturbances and tasks, which are described in the following subsections and mainly follow the approaches from [1].

A. Detumbling

After orbital injection, the spacecraft may tumble in an uncontrolled manner, requiring the ADCS to counteract the

initial angular momentum to enable proper operation. Thus, the actuators must be designed to meet the detumbling requirement see Table XXVIII. To calculate the required detumbling torque within one orbit, the angular acceleration is computed by:

$$\dot{\omega} = \frac{\Delta\omega}{T_{orbit}} \tag{19}$$

$\dot{\omega}$ is the angular acceleration, ω is the initial tumbling rate of the satellite, T_{orbit} the orbit time. With the computed angular acceleration the required torque to detumble can be calculated by:

$$T_{detumble} = I * \dot{\omega} \tag{20}$$

$T_{detumble}$ is the torque required to detumble, I is the moment of inertia of the spacecraft. The required magnetic dipole moment to generate the detumbling torque is calculated by:

$$m = \frac{T_{detumble}}{B} \tag{21}$$

m is the magnetic dipole moment, B is the Earth's magnetic field strength. For the calculations, an initial tumbling rate of $\omega = 5.7\frac{^\circ}{s}$ was assumed, the spacecraft is considered to be detumbled when its angular velocity is lower than $\omega = 0.13\frac{^\circ}{s}$ [33]. To design the ADCS for the satellite in this project, the moment of inertia was derived directly from the CAD model of the entire satellite. It is important to note that during the initial tumbling phase, which is caused by orbit injection, the solar arrays are not yet deployed. As a result, the moment of inertia matrix of the satellite differs between the initial tumbling phase and later operational phases when the solar arrays are deployed.

B. Slew Torque - Falk

In order to guarantee effective maneuverability of the satellite, it is essential that the actuators are able to meet the slew requirement of the ADCS. This requirement states that the ADCS shall be capable of rotating the spacecraft along each axis at a minimum slew rate of 0.25°/s see Table XXVIII. The slew rate of 0.25°/s represents that the satellite should be able to turn 15° around each axis in a time period of one minute. Therefore, the required slew torque can be calculated with the following formula from [1]

$$T_{slew} = 4\Theta\frac{I}{t^2} \tag{22}$$

Θ represents the turning angle, I is the moment of inertia of the spacecraft, t is the time required for the slew.
The momentum change during the slew maneuver is calculated by:

$$h_{slew} = T_{slew}\frac{t}{2} \tag{23}$$

h_{slew} is the total momentum change, T_{slew} is the slew torque, t the required time.
For the slew torque calculations, it was assumed that the solar arrays are now fully deployed. Consequently, the moment of inertia differs from the one used for the detumbling calculations. The moments of inertia, again, were obtained from the CAD model.

C. Environmental Disturbances - Falk

In low-Earth orbits, spacecrafts encounter various environmental disturbances causing forces and torques which can lead to undesired satellite movements. The ADCS has to counteract these disturbances to ensure proper satellite operation. This project specifically addresses several notable perturbations: aerodynamic drag, Earth's magnetic field, solar radiation pressure, and the Earth's gravity gradient. Other additional perturbations like micrometeorites and third-body gravitational effects are not considered in this project due to their relatively minor minor impact. The Table VIII shows the magnitude of the calculated different disturbance torques. Further explanations on how these disturbances were calculated can be found in the appendix section XVI.

TABLE VIII
DISTURBING TORQUES SUFFERED BY THE SATELLITE

Torque Type	Value [Nm]
Atmospheric drag	$0.1426\ 10^{-5}$
Gravity gradient	$0.0186\ 10^{-5}$
Solar radiation pressure	$0.0044\ 10^{-5}$
Magnetic Field	$0.4390\ 10^{-5}$

D. Pointing - Falk

To achieve the precise pointing accuracy of 0.1° for the high-precision camera payload, the ADCS design must guarantee that the actuators and sensors can meet this requirement. Therefore, the combined sensor resolution should be capable of determining the satellite's attitude within an additional margin of the required accuracy. More information about the sensor selection is provided in subsection IX-H. In addition, the actuators must be designed to steer the satellite to the desired attitude within a the required range of accuracy. Thus, reaction wheels are selected as actuators due to their capability to provide precise pointing [1]. Details on the actuator selection is provided in subsection IX-E.

E. Actuators - Falk

In order to maneuver and reorient the spacecraft while countering external and internal forces, actuators are required. The primary types of satellite actuators include thrusters, reaction and momentum wheels, control moment gyros(CMG), and magnetorquers. In the designing process of the satellite, a 6U CubeSat was depicted as the overall size, considering the selected payload and orbit. Consequently, the selected actuators need to meet the maneuverability and detumbling requirements while aligning with the spacecraft's overall design and size. Thrusters offer versatility, as they function in various orbits and altitudes, and can generate torques about any axis. However, a significantly throwback, especially for smaller satellites, is that they require fuel and might have

problems in counteracting small disturbances for precise pointing accuracy due to limitations of providing small impulses. Control moment gyroscpes (CMG) provide greater accuracy but tend to be larger and heavier due to their complex functionality[34]. Thus, magnetorquers and reaction wheels are selected as the most suitable actuators for the presented satellite design. The following Table IX shows the required torques and corresponding capacities which served as the basis for the actuator selection.

TABLE IX
MAXIMUM TORQUES FOR EACH PART OF THE SYSTEM

Item	Value
Torque required for detumbling	$0.1729\ 10^{-5}$ Nm
Torque required for slew maneuver	$7.4264\ 10^{-5}$ Nm
Momentum storage for detumbling	0.01 Nms
Momentum storage for slew maneuver	$2.4755\ 10^{-6}$
Magnetic dipole for detumbling	$0.0394\ Am^2$

1) Reaction Wheels: With respect to the required torques, capacities and the pointing accuracy, the reaction wheels "CubeWheel - M" from the company CubeStar were selected. A brief overview of the parameters are shown in the Table X. The chosen reaction wheels were selected as they offer

TABLE X
REACTION WHEEL - CUBEWHEEL M

Parameter	Value
Speed Range	6000 RPM
Max Momentum	10.8 mNms
Max Torque	1.0 mNm
Mass	150 g
Average Power	190 mW

an appealing combination of high momentum capacity, low power consumption and low mass, with proven flight reliability. Three of those reaction wheels were strategically positioned along the principle axis and satellite's centre of mass to optimize control authority. For redundancy, an additional reaction wheel was considered to avoid single-point failures. Typically, four reaction wheels are mounted either in pyramid or in NASA standard configuration, ensuring that if one wheel fails, the remaining three can still control the satellite across all axes. More information on reaction wheels placement can be found in the cited paper [35]. However, due to the inclined placement of the reaction wheels, additional momentum capacity might be necessary [1]. Moreover, the redundant wheel adds weight and requires space, critical factors for CubeSats. Furthermore, four reaction wheels increase the control complexity as it is an over-determined system. Considering these factors, a trade-off was made against incorporating a redundant fourth reaction wheel, since magnetorquers are also part of the actuator selection.

2) Magnetorquers: In addition to reaction wheels, magnetorquers were also selected as actuators for the satellite. While reaction wheels are mainly for fine attitude adjustments, magnetorquers are used for detumbling the satellite after orbit deployment and for desaturating the reaction wheels if needed. Three CubeTorquer M from CubeSpace were selected as they fulfill the required torque specifications, are already flight-proven, and are aligning within our mission's need. Table XI below shows an overview of the selected magnetorquers, presenting key parameters.

TABLE XI
MAGNETORQUER - CUBETORQUER M GEN 1

Parameter	Value
Minimum magnetic moment	0.66 Am²
Magnetic Gain	8.2 Am²/A
Mass	36 g
Max Current	150 mA

F. Desaturation - Falk

Due to the selection of reaction wheels as actuators, it is crucial to have the capability to desaturate them. Reaction wheels function by storing momentum, which means that they accumulate angular momentum due to their rotational motion. However, over time, the reaction wheels may reach a maximum angular velocity, preventing them from further absorbing angular momentum in that direction. As a consequence, other actuators must be activated to generate torques in the opposite direction of the reaction wheel's rotation. During this process(called desaturation) the reaction wheel is counteracting the generated torque, causing a reduction in its accumulated momentum, allowing it to resume to its normal operations and accumulate angular momentum in both directions again. As described in subsection IX-E reaction wheels and magnetorquers are selected as actuators for this satellite mission. Therefore, it is essential that the magnetorquers are able to desaturate the reaction wheels. This means they need to generate an angular momentum equal in magnitude to the maximum stored angular momentum of the reaction wheels in order to fully desaturate them. The required angular momentum for desaturation is specified in the Table X, corresponding to the capacity of the reaction wheels. To calculate the torque that the magnetorquers provide, the following formulas are used:

$$m = M * I \tag{24}$$

$$T_{mt} = m * B \tag{25}$$

m is the magnetic dipole moment generated by the magnetorquers, M is the magnetic moment of the magnetorquer, I it the current flowing through the magnetorquer, T_{mt} is the torque produced by the magnetorquer interacting with Earth's magnetic field which is represented by B. A first estimation of time required to desaturate fully the reaction wheels can than be calculated by:

$$t_{desat} = \frac{L}{T_{mt}} \tag{26}$$

t_{desat} is the time required for desaturate the reaction wheels, L is the angular momentum storage and T_{mt} is the torque provided by the magnetorquer. To satisfy the desaturating

requirement see Table XXVIII, t_{desat} needs to be smaller than the orbit period.

G. ADCS CubeSystem - Falk

During the ADCS design phase, after selecting the actuators (reaction wheels and magnetorquers), it was considered to use a fully integrated ADCS. CubeSpace offers such a solution with the already pre-selected actuators. The advantages of an integrated ADCS are that it ensures proper compatibility and comes with an ADCS onboard computer. Moreover, the ADCS CubeSystem fits into one U and is already flight proven. Regarding those advantages, we opted for the CubeSystem from CubeStar as the ADCS for the satellite and to selected the available options regarding our mission's requirements. CubeSpace offers three different control types for the CubeADCS of which the 3-axis solution was selected. The Table XII provides an overview about the CubeSystem configuration. In subsection IX-H the sensor selection is further explained.

TABLE XII
SUBSYSTEMS OF THE ADCS CUBESYSTEM

Item	Product name
Reaction wheels	CubeWheel M x3
Magetorquers	CubeTorquer M x3
Star Tracker	CubeStar x1
Sun Sensor	Coarse Sun Sensor x10
Magnetometer	CubeMag deployable x1 CubeMag redundant x1
Horizon sensor	CubeSense x1

For more in-depth insights about the ADCS subsystems, the CubeADCS documentation is recommended [14]. Calculation were made with MATLAB which prove that the selected actuators satisfy the ADCS requirements.

H. Sensors - Falk

For determining the attitude of the satellite different sensors are required. There is wide range of sensors which use different measure approaches to determine the attitude of the satellite. Thus, they are different in size, accuracy and costs. In the following section, we will focus on explaining the specific sensors utilized in this project. For information on additional sensors, the SMAD book can be referenced for further details [1].
The selected sensors are described in Table XIII. Further information about each sensor can be found in their documentation [14]

TABLE XIII
SENSOR SELECTION

Sensor	Accuracy	Num.
Star Tracker	$< 0.0154°$	1
Sun sensor	$< 10°$	10
Magnetometer	$< 50nT$	2
Horizon sensor	$< 0.22°$	1

1) Star Tracker: Star sensors, on 3-axis stabilized systems commonly used as star trackers, are considered the most accurate reference sensors. These trackers capture and process images to identify and track stars based on a star catalog and thereby provide a 3-axis attitude determination of the satellite. Due to the high number of stars, sophisticated techniques are required in the instruments, thus making star trackers relatively expensive, power-hungry, and massive [34]. Additionally, they necessitate some initial knowledge of the satellite's attitude and may have strict operational limitations like rate restrictions. However, given the stringent accuracy requirement, a miniature, low-power, medium accuracy star tracker from CubeStar is selected for the ADCS [14]. The CubeStar - Gen 1, though medium accuracy, exhibits the necessary precision of $< 0.1°$, making it suitable for the mission. However, due to the maximum slew rate of $0.3\frac{°}{s}$, additional sensors are required, particularly during the initial tumbling phase.

2) Sun Sensor: Sun sensors measure one or two angles between the incident sunlight and their base, providing reliable measurements with varying levels of accuracy, ranging from coarse sun sensors to high precision levels below $0.01°$ [1]. For this satellite, several very coarse sun sensors from CubeSpace are selected, due to their small size affordability, and low power consumption. To ensure functionality, ten of these coarse sun sensors are strategically positioned around all sides of the satellite's surface, with at least six sensors receiving a sun vector during the sunlit portion of the orbit, as required CubeSpace [14]. The additional sensors provide redundancy and account for potential shadowing or obstruction. Although the selected sun sensors only offer a rough estimation of the satellite's attitude, they still provide initial knowledge of the satellite's position, facilitating the star tracker's operation.

3) Magnetometer: Magnetometers are sensors which measure the Earth's magnetic field, direction and intensity to determine the spacecraft's attitude relative to it. Although they are known for their simplicity, reliability and lightweight design, their accuracy is limited [1]. Nevertheless, since magnetic torquers are chosen as actuators, magnetometer play a crucial role in controlling the torquers output magnitude and direction. Therefore, the magnetometers CubeMag from CubeSpace are selected as additional sensors to ensure the proper functioning of the magnetorquers. Moreover, an additional magentorquer is incorporated to enhance system redundancy and overall mission robustness.

4) Horizon Sensor: Earth's horizon sensors are another common sensor to determine a spacecraft's attitude. They determine the nadir vector by sensing the position of Earth's horizon and are usually designed to operate in infra-red [34]. By capturing the intensity of the light between the Earth's surface and the void of space, they can determine the spacecraft's attitude relative to Earth. While the combinations

of star tracker, sun sensors and magnetometer might already be able to determine the attitude of the satellites within the required accuracy, an additional horizon sensor is included for redundancy and overall robustness of the system.

I. Mass Budget

The mass budget can be obtained by adding up the distinct masses of the different subsystems. The IX-I presents the different masses of each subsystem and its contribution the overall dry mass of the satellite. The total launch mass sums up to $10.0kg$ which allows an additional margin of 20% until reaching the maximum weight of 12kg for a 6U CubeSat[36].

TABLE XIV
MASS BUDGET

Subsystem	Mass [kg]	% of Dry Mass
Structure	3.00	30.64
Payload	0.44	4.49
Power	2.32	23.70
Communications	2.00	20.43
ADCS	0.85	8.68
Onboard Computer	0.50	5.11
Propulsion	0.68	6.95
Total Dry Mass	**9.79**	**100**
Propellant	0.22	2.25
Total Launch Mass	**10.01**	**102.25**

X. Launcher and Launch Site Selection

A. Launcher - Anibal & Ditsa

A satellite rocket launcher, also known as a launch vehicle or a rocket, is a vehicle designed to propel satellites into the space. It is responsible for delivering the satellite to its desired orbit around the Earth or other celestial bodies. A comparative study was done with respect to the different types of launchers which are designed by different space agencies and private companies worldwide and the final choice was made to select Falcon 9's SmallSat Rideshare Program as the best option with respect to our mission. The Falcon 9 SmallSat Rideshare Program is an initiative introduced by SpaceX to provide affordable access to space for small satellites like CubeSats which are often used for research, educational and technology demonstration purposes [37]. Below are some of the reasons as to why this option is the most feasible one.

1) Shared Payloads: SpaceX's Falcon 9 rocket is primarily designed to deliver larger payloads, such as communication satellites or resupply missions to the International Space Station (ISS). However, there is often extra space available on these missions, which can be utilized for smaller payloads like CubeSats. The Falcon 9 Rideshare Program allows multiple CubeSats to be launched together, sharing the same launch vehicle [38].

2) Cost Efficiency: By sharing the launch with other payloads, CubeSat operators can benefit from significant cost savings. Traditionally, securing a dedicated rocket launch can be prohibitively expensive for small satellite operators. The rideshare program provides an affordable alternative, allowing multiple CubeSats to reach space at a fraction of the cost compared to a dedicated launch.

3) Dispenser System: To accommodate the CubeSats within the Falcon 9 rocket, SpaceX employs a dedicated dispenser system called the Payload Stack Adapter (PSA). The PSA is a structure that holds the CubeSats in a stacked configuration, ensuring their safe deployment into space [38].

4) Sun-Synchronous Orbits: The Falcon 9 rideshare program typically launches CubeSats into SSO. SSOs are a specific type of orbit that allows satellites to pass over any given point on Earth at the same local solar time during each orbit. This orbit is commonly used for Earth observation missions, as it ensures consistent lighting conditions for imaging.

5) Deployment Mechanism: Once the Falcon 9 reaches the desired orbit, the CubeSats are deployed into space by a deployment mechanism which can release multiple CubeSats simultaneously. An ensured, controlled and precise deployment process is carried out, minimizing the risk of collision or interference between the CubeSats.

The following Table XV shows some specifications regarding the launcher Falcon 9.

TABLE XV
FALCON 9 SPECIFICATIONS [39]

Parameter	Value
Manufacturer	SpaceX
Diameter	3.7m
Total Height	70m
Liftoff Mass	550t
Operating since	2010
Orbital Inclination at LEO	28.5°
Stages	2
Propellant System	RP-1, LOX
Orbits	LEO, SSO, GTO, Polar

B. Launch Site - Ditsa

Vandenberg Space Force Base, located in California, USA, is considered an ideal launch site for the Falcon 9. It is one of the top four rocket launch sites in the United States, along with Cape Canaveral Space Force Station, Kennedy Space Center, and the Wallops Flight Facility. Satellites with an orbital inclination of more than 56 degrees could not be launched from Cape Canaveral launch site, as the rockets had to fly over the mainland instead of the sea stretch. Hence, a new location for another base was looked upon eventually, specifically suitable for polar orbits and sun-synchronous orbits. Vandenberg is situated in the south of the US, details of which further will be explained below, and is in an azimuth range of 158° to 201°. This results in possible web inclinations of 70° to 104° [40]. As our mission has the aim of reaching an orbital inclination of approximately 97°, this launching site is well suited for our mission as well. This is an ideal launch site for the Falcon 9 rocket for several reasons as follows:

1) Orbit launches: Vandenberg is one of the few locations in the United States that allows rockets to launch into polar orbits. Polar orbits are crucial for many Earth observation and

remote sensing satellites as they provide global coverage and pass over the Earth's poles, capturing images and data from all latitudes [40].

2) Favorable Geographical Position: Vandenberg is well-positioned geographically for various orbital inclinations, which are the angles of a satellite's orbit relative to the equator. This allows Falcon 9 to efficiently access a wide range of orbits, including polar, sun-synchronous, and other inclined orbits.

3) Environmental Considerations: Launching from Vandenberg can minimize the environmental impact on land as most of the rocket's trajectory occurs over the ocean. This reduces the potential for noise disturbances and other environmental concerns often associated with launches from inland sites.

4) Launch Frequency and Scheduling: Vandenberg's infrastructure and operational capabilities enable it to accommodate a relatively high launch frequency. This allows SpaceX to maintain a busy launch schedule, meet customer demands, and provide more opportunities for satellite deployment [40].

C. Orbital Transfer Vehicle - Anibal

Launchers are designed to carry payloads from Earth's surface into space. The specific destination they take payloads to depends on the mission requirements and objectives. Choosing a rideshare option for launching a 6U satellite can offer several benefits such as cost-effectiveness, faster deployment, and reliability. Nevertheless, rideshare programs come with certain issues that must be addressed. As the launch carries multiple payloads, this means that the primary payload determines the orbit and trajectory of the mission. Secondary payloads such as smaller spacecraft may need to compromise on their desired orbits or deployment timings. This lack of flexibility can be a significant drawback.

To overcome these challenges, employing an Orbital Transfer Vehicle (OTV) becomes a compelling solution. An OTV serves as an intermediary spacecraft capable of performing orbital maneuvers, transporting payloads to their desired destinations. The OTV can take advantage of its dedicated propulsion system to perform multiple orbital transfers, gradually adjusting the inclination and altitude, approaching the desired orbit. This, in turn, reduces the dependency on the primary payload's schedule, enabling a more tailored and reliable deployment strategy for the secondary payload.

1) Exolaunch GmbH Overview: Exolaunch GmbH is a reputable provider of launch, deployment, mission management, and integration services for NewSpace actors. With a successful track record of supporting over 320 satellites across 21 missions, Exolaunch has collaborated with numerous international smallsat operators, research centers, and universities [41]. The company has strong academic roots, being a spin-off of the Technical University of Berlin, and maintains close ties with academia, launching more than 80% of all German universities and research centers' satellites. Moreover, Exolaunch has a great experience of working with the Technical University of Munich in the framework of the *MOVE-II* project that was launched on a Falcon 9 in December 2018 [42].

2) Launch Proposal Details: Having contacted Exolaunch, and as stated in subsection X-B, the following launch details were proposed:

- **Timeline**: Q4 2025
- **Orbital Parameters**: 500-600km, Inclination SSO
- **Satellite Form Factor**: 6U CubeSat
- **Separation System**: EXOpod CubeSat deployer
- **Launch Vehicle**: SpaceX Falcon 9
- **ROM Price (EUR)**: 215.000

SpaceX has a multi-year *Multi-Launch Agreement* with Exolaunch providing authorization to Exolaunch to integrate small satellites for Falcon 9 missions. Since 2020, Exolaunch has launched over 220 smallsats with Falcon 9, for customers such as Planet, ICEYE, Satellogic, NanoAvionics, DLR, Swarm, Loft Orbital, and Spire. [42]

3) EXOpod Nova CubeSat Deployer: The EXOpod Nova CubeSat Deployer is a state-of-the-art separation system, built on years of experience working with leading cubesat developers and launch providers, and is set to redefine the term "cubesat". Nova offers up to four times more space for lateral protrusions, while also increasing the possible mass capacity by up to 33% compared to other deployers on the market. Building on the significant flight heritage and inheriting the best features of EXOpod, Nova adds new capabilities, boosts performance, and further increases reliability. EXOpod Nova has several features which expand the limits of the *Cubesat Design Specification (CDS)*:

- **Compatible**: Easily adaptable to any launch vehicle.
- **Clamping Mechanism**: Cubesats inside EXOpod Nova are secured in place once the door is closed.
- **Flexible**: EXOpods have been used for cubesats ranging from 0.25U to 16U in size. The EXOpod Nova has deployed 3U and 6U cubesats on its maiden flight in May 2022. More than 25 Novas will have been flown before Q1 2024, deploying cubesats between 1U and 16U in size.
- **Fast Reset Time**: The EXOpod Nova can be deployed and locked again in minutes.
- **Increase Available Mass**: Cubesats in an EXOpod Nova can be heavier than CDS limits.
- **Access Windows**: Windows on at least two sides of the deployer provide access to the cubesat within, useful for inspection, testing, and RBF pin removal after integration.
- **Flight Heritage**: EXOpods have been used on 15 missions to launch and deploy 202 cubesats since 2017. EXOpod Nova has successfully flown for the first time in Mai 2022 deploying 5 satellites. 24+ units are anticipated to fly before Q1 2024.
- **ITAR-Free, Made in Germany**: The system is not subject to export restrictions of any kind.

All the above information has been provided through a proposal of a contractual agreement pursued by Anibal Guerrero

and as such, is valid until October 31, 2023, simulating how a real agreement would take place.

XI. Tracking, Telemetry, and Control System - Rakesh

Every spacecraft needs a communication subsystem to transmit data generated by the payload and exchange data associated with Tracking, Telemetry, and Control. The telemetry data relates to the health status of spacecraft through the collection, processing, and transmission of data from the various spacecraft subsystems. The tracking data consists of the satellite's exact location, whereas the control data contains commands from the ground station to the satellite [1].

A. Frequency Selection and Licensing - Rakesh

Initially, the operating frequency for the communication subsystem needs to be selected concerning data exchange with the ground station. Direct communication with the ground station provides a meagre communication time of 7 to 9 minutes for any arbitrary satellite in Lower Earth Orbit (LEO) and proposing multiple ground stations would result in higher operational costs. Furthermore, spatial crowding of frequency in lower bands (L & S-bands) has caused problems with frequency licensing and using higher frequency bands (Ku, K & Ka-bands) results in significant atmospheric signal power losses. To compensate for multiple losses, a heavy high-gain antenna is required. Hence, a relay satellite system was proposed for communicating with a single ground station to achieve a high data rate with a smaller antenna. This results in saving operational costs, satellite mass and ease in frequency licensing.

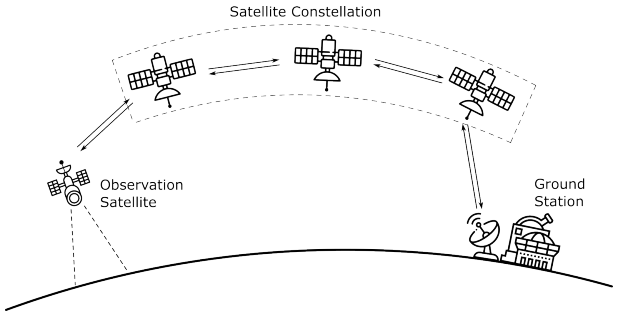

Fig. 6. Data relay through Satellite Constellation

After reviewing different existing and proposed satellite constellations that provide data relay services in a few years, the Telesat Lightspeed™ satellite constellation was selected. Telesat Lightspeed™ satellite constellation was chosen due to following reasons:

1) Telesat Lightspeed™ satellite constellation will orbit in LEO between 1000 to 1300km [43], which is higher than the selected orbit of our satellite. Also, the spatial distance between our satellite and the constellation is low, reducing free space losses.
2) Telesat Lightspeed™ satellite constellation is being designed with Ka-band and optical inter-satellite link (OSL), which reduces latency and allows high data rates [43].
3) Telesat Lightspeed™ satellite constellation has been planned for over 180 satellites. This will result in reliable and prolonged communication between our satellite and the ground station [43].

The licensing of the frequencies will be carried out by the following [44] and [45].

TABLE XVI
Frequency Selection

	TT&C Subsystem	**Telesat Lightspeed™ Satellite**
Transmitter Antenna	17 - 21 GHz	27.5 - 29.1 GHz & 29.5 - 30.0 GHz [43]
Receiver Antenna	27 - 30 GHz	17.8 - 18.6 GHz & 18.8 - 20.2 GHz [43]

B. Component Selection - Rakesh

The communication subsystem generally comprises the antenna(s), a transmitter, and a receiver. The transmitter converts the digital data into an analog signal via different signal processing and sends it to the antenna for transmission, whereas the receiver converts the analog signal from the antenna to digital data.

After reviewing different antennas and associated transmitters and receivers, we decided to use a transponder. A transponder is a complete solution, including antenna(s), transmitter, and receiver modules. Following this thought, a Ka-band transponder is used with the specification given in Table XVII.

TABLE XVII
Transponder Specification[13]

Parameters	**Specifications**
Name	ReliaSat KKa-TRSP-1929
TX output frequency	17 - 21 GHz
RX input frequency	27 - 30 GHz
Saturated output power	27 dBm
Tx conversion gain	38 - 43 dB
Noise figure	< 2.5 dB

Figure 7 shows the transmitter's upconverter and the receiver's downconverter operating in different frequency bands. The transponder has multiple Bandpass Filters, High-pass Filters and Low-pass Filters for filtering the noise in the signal. Gain blocks and amplifiers are used to increase the signal power level. The mixers are used for the modulation and demodulation of the information signal in the carrier signal.

C. Modulation and Coding Scheme - Rakesh

The information from the satellite is carried using a carrier signal. This is done via modulation. Similarly, demodulation

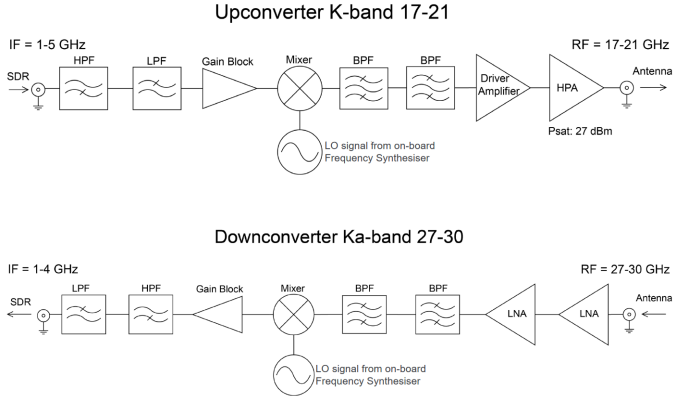

Fig. 7. Upconverter & Downconverter of KKa-TRSP-1929

is the process of recovering information from the receiver signal. The modulation of a signal is carried out using a coding scheme. There are various coding schemes depending on the type of modulation used. For our purpose, the Phase-Shift Keying (PSK) modulation technique is used as it has higher spectral efficiency (bps/Hz) and Bit Energy E_b than amplitude and frequency modulation [1]. Although high-order PSK modulation up to 16 phases state per symbol is achievable to increase spectral efficiency, it also increases the susceptibility of communications links to phase-noise-induced error, also known as Bite Error Rate.

After performing the link budget see Table XVIII and calculating the available energy-to-noise ratio (E_b/N_o) of the link, the coding scheme of 8PSK is selected [1]. And for detailed Link Budget, refer to Table XXIX.

TABLE XVIII
LINK BUDGET - RAKESH [XXIX]

Link Parameters	Value	Units	Notes
Uplink Frequency	27	GHz	Telesat to the CubeSat
Available E_b/N_o, Uplink	15.42	fdB-Hz	Table XXIX
Downlink Frequency	17.8	GHz	CubeSat to Telesat
Available E_b/N_o, Downlink	93.90	dB-Hz	Table XXIX
End-to-End E_b/N_o	15.42	dB	Uplink plus Downlink
Modem Implementation Loss	-1.2	dB	Representative for this scenario [1]
Required E_b/N_o	5.41	dB	[1] Table 16-12
Link Margin	8.81	dB	
Single User Data Rate	44	Mbps	
Code Rate, ρ	5/6		For 8-PSK,[1] Table 16-12
Single User Bandwidth	35.376	MHz	
BER	4.51E-08		For 8-PSK, [1] Fig 16-16
Error Bits	0.188		
Error Pixels	0.0236		

XII. GROUNDSTATION - DITSA

A satellite ground station, also known as a ground terminal or earth station, is a facility that communicates with satellites in orbit. It serves as a crucial link between satellites and various terrestrial networks, enabling the exchange of data, commands, and other information between the satellite and the ground-based infrastructure. There are several important requirements to consider when choosing a ground station for a satellite spacecraft like a CubeSat like **frequency band**, **antenna system**, **location**, **licensing and regulatory considerations**, **groundstation capabilities**, **communication protocols**, **ground station operator support** and **cost and accessibility**.

From the Table XVI and Table XVII in the previous section, the frequency bands as well as the antenna system has been decided and fixed for our mission respectively. Keeping them in mind, **the DLR ground station in Weilheim**, has been selected. It is located around 60kms south-west of Munich, Germany. Inaugurated in the year 1968 and established in 1969, this groundstation is operated by the DLR German Space Operations Center (GSOC). It can support space missions in the **L, S, X, Ku, and Ka frequency bands.** The station facilities as well as the antennas are controlled and monitored from a single common control room. It operates 24 hours, 7 days a week. A small overview of the antennas corresponding to our mission in Weilheim which are known to be used for the various Multi-Mission operations is provided below in Table XIX [46].

TABLE XIX
WEILHEIM ANTENNAS [46]

Parameter	Antenna 1	Antenna 2
Designation	13m	11m
GDS Name	S73	S70
Band	Ka	Ku
Freq [GHz] (R)	$18,1-21,2$ $25,2-27,5$	$10,70-12,75$
Freq [GHz] (T)	$22,55-23,15$ $27,5-31,0$	$13,75-14,50$
Pointing Accuracy	$\pm 0,001$	$\pm 0,01$

Factors like environmental conditions can impact satellite ground stations through factors like extreme weather events, solar radiation interference, electromagnetic interference, ground stability issues, vegetation obstruction, wildlife interference, corrosion, seismic activity, and power supply disruptions. The following Table XX shows some insights with regard to the environmental conditions at the DLR ground station in Weilheim.

When considering political stability as a factor in choosing a satellite ground station location, Germany is known for its stable political environment, with a strong democratic system and well-established institutions. It is a member of the European Union (EU), which promotes cooperation and stability among its member states. Its commitment to multilateralism and international cooperation can be beneficial for satellite missions involving global collaboration. The country's regulatory framework for satellite communications and space activities is typically transparent and well-defined.

TABLE XX
ENVIRONMENTAL CONDITIONS OF WEILHEIM GROUNDSTATION [46]

Parameter	Operational Conditions	Survival Conditions
Outside Temp. [°C]	-30 to 50	-35 to 60
Inside Eqpmt [°C]	0 to 40	N/A
Wind	$\leq$ 75km/h	$\leq$ 200km/h
Degraded Perf.	$\leq$ 120km/h	N/A
Rain	100mm/h	N/A
Snow	$\leq$ 30mm/h	$\leq$ 100mm/h
Ice	$\leq$ 5mm	$\leq$ 30mm
Humidity	$\leq$ 100%	N/A
Solar Radiation	1kW/m2	N/A
Seismic	N/A	0, 3g (H), 0, 1g (V)

XIII. PROPULSION SYSTEM - ANIBAL

In recent years, the space industry has witnessed a major transformation in satellite propulsion systems, with a significant shift toward more efficient and adaptable technology. The inclusion of Electric Propulsion Systems (EPS) has emerged as a major changer, particularly for 6U CubeSats. As the need for small, low-cost satellite missions develops, EPS offers an unprecedented solution that promises better agility, longer mission lives, and access to a broader selection of orbital destinations.

A. Propulsion System Requirements - Anibal

The propulsion system's main function is to carry out station-keeping maneuvers, ensuring that the spacecraft's orbit does not degrade more than 30km from the desired orbit planned for the spacecraft. This will enable it to maintain its position within the specified orbital parameters as contemplated in section VII, resulting in a precise and consistent Earth observation data collection.

The propulsion system's architecture has a great influence on the spacecraft's capabilities. Therefore, it is essential to choose an appropriate architecture.

B. Assumptions, Trade-offs, Justification, and Impact - Anibal

To do so, a *trade-off analysis* is performed. The analysis adheres to the European Cooperation for Space Standardization (ECSS) regulations, specifically:

- **ECSS-E-ST-35C Rev. 1 Space engineering**: Propulsion general requirements
- **ECSS-E-ST-35-01C Space engineering**: Liquid and electric propulsion for spacecrafts

This trade-off analysis involves a step-by-step evaluation of various relevant parameters to ensure that the chosen propulsion system architecture meets the specific mission requirements effectively. The following steps were followed in the trade-off analysis:

1) **Propellant system's technical data**: select pertinent parameters to evaluate the performance of each propulsion system architecture.
2) **Parameter relevance for the mission**: assign a relevance score to each parameter, indicating its importance in the mission.
3) **Parameter criteria**: define specific ranges for each parameter.
4) **Criteria assignment to each propulsion system architecture**: a score from 1 to 5 is assigned to each parameter for each architecture.
5) **Score calculation**: scores are assigned to each parameter weighted with their relevance scores.
6) **Final scores**: total scores are summed up for each architecture.

1) Propellant System's Technical Data: The parameters chosen are based on their relevance to the mission's objectives and their impact on the propulsion system's performance and overall mission success. The chosen parameters include:

- **Performance**: Specific Impulse (Isp), Thrust
- **Mission Requirements**: Mission Duration (T mission), Re-ignitability
- **Resulting Layout**: System Complexity, Total Mass & Volume, Required Power
- **Compatibility and Contamination**: System Compatibility, Contamination Risk
- **Experience**: Technology Status
- **Availability of Components**: Component Availability, Total Cost

Table XXIII gathers all the relevant data corresponding to each parameter.

2) Parameter relevance for the mission: By ranking these parameters in order of importance, the trade-off analysis aims to guide the selection of the most suitable propulsion system architecture for the mission. Each parameter's significance is carefully evaluated to ensure that the chosen propulsion system aligns with the mission's specific requirements and constraints, ultimately enhancing the mission's chances of success. These have been ranked in order of importance in Appendix G, subsection XVI-G.

Additionally, these relevance scores are reflected in the grading system included in Table XXIV.

3) Parameter criteria: The third step entails defining specific criteria or acceptable ranges for each parameter. This step is essential to establish clear guidelines for evaluating the performance of each propulsion system architecture. By determining the minimum and maximum values within which each parameter should ideally fall, the analysis ensures that the propulsion systems meet the mission's requirements effectively. For instance, in the case of *Specific Impulse*, a specified acceptable range would ensure that the propulsion system's efficiency is sufficient to carry out the orbital maneuvers in a timely manner.

These criteria are reflected in Table XXV.

4) Criteria assignment to each propulsion system architecture: Having defined the criteria, a score from 1 to 5 is assigned to each parameter for each propulsion system architecture. This scoring process is based on how well each parameter performs within its specified range. Higher scores are granted to architectures that excel in meeting the established criteria, indicating their better suitability for the

mission. For example, if a propulsion system demonstrates it has been flight proven, it would receive a higher score under the *Technology Status* than another propulsion system that is still being developed.

These criteria assignments are reflected in Table XXVI.

5) Score calculation: The next step involves weighting the scores assigned to each parameter based on their relevance to the mission. Relevance scores, previously assigned in the second step, reflect the importance of each parameter in the context of the mission. Parameters with higher relevance receive greater weight, signifying their greater influence on the overall assessment of each propulsion system architecture. This ensures that critical parameters, such as *Total Mass & Volume* and *Technology Status*, have a more significant impact on the final evaluation, reflecting their crucial role in meeting mission objectives.

The scores can be seen in Table XXVII.

6) Final scores: Finally, the total scores for each propulsion system architecture are summed up to calculate the overall score in Table XXVII. These final scores represent the propulsion systems' overall performance and suitability in meeting the mission's specific requirements. The propulsion system with the highest final score is considered the most suitable choice for the mission, aligning well with the mission's goals and constraints. In this case, the best propulsion system architecture is **electrostatic**.

TABLE XXI
TRADE-OFF ANALYSIS - FINAL SCORES

Propulsion System	**SCORE**
Hybrid	2.99
Liquid Monopropellant	2.98
Liquid Bipropellant	3.29
Electrostatic	3.46
Electromagnetic	3.14
Nuclear	2.64
Other(Solar Sail)	3.19

C. System Architecture and Design Decision - Anibal

After conducting an exhaustive and comprehensive evaluation of various propulsion options suitable for our mission, which involved considering high-thrust bi-propellant thrusters for quick orbital adjustments, we encountered challenges related to the increased mass of the satellite. In order to arrive at an optimal solution, we conducted an extensive trade-off analysis, considering our mission requirements, particularly the need for effective station-keeping maneuvers. As a result of this rigorous evaluation process, Table XXI, we have strategically decided to adopt the electrostatic propulsion system for our 6U satellite. The selection of the electrostatic propulsion system represents a significant advancement in propulsion technology and offers a tailored and unique alternative, specifically designed for smaller space missions such as CubeSats. This system places special emphasis on efficiency and maneuverability, which are crucial for the success of our mission. By utilizing electric fields to accelerate charged particles, this cutting-edge propulsion technology yields a higher specific impulse and significantly reduces the constraints imposed by propellant mass. The key objective behind implementing the electrostatic propulsion system is to maximize mission efficiency while overcoming the limitations posed by conventional bi-propellant thrusters. This decision instils confidence in our ability to achieve precise station-keeping, optimize satellite performance, and successfully carry out our mission objectives with increased efficiency and reliability.

D. Thruster Selection - Anibal & Danica

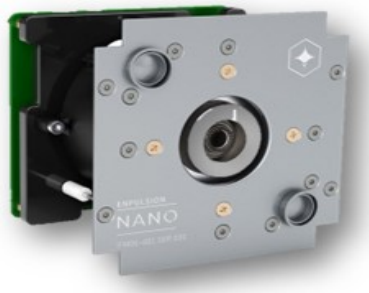

Fig. 8. Enpulsion Nano [17]

After careful consideration of various propulsion options, we have made a definitive choice in selecting the ENPULSION NANO thruster Figure 8 as the optimal solution to meet the propulsion requirements of our mission [17]. The compact size of this thruster not only facilitates seamless integration but also plays a pivotal role in achieving a balanced payload distribution, essential for adhering to the overall weight constraints of our satellite. One of the key factors influencing our decision is the incorporation of Field Emission Electric Propulsion (FEEP) technology within the NANO thruster. This cutting-edge technology is renowned for its exceptional specific impulse and efficiency, aligning perfectly with our mission objective to minimize propellant mass while extending the duration and operational capabilities of the satellite. By harnessing the benefits of FEEP technology, we can significantly extend the lifespan of our mission, allowing us to gather more valuable data and enhance our satellite's functionality during its time in space. Another crucial advantage of the NANO thruster lies in its remarkable precision, enabling us to conduct station-keeping maneuvers with enhanced accuracy and control. This capability is of utmost importance in ensuring our satellite maintains its designated orbital position, thus avoiding potential collisions and optimizing communication with ground stations. The enhanced station-keeping performance offered by the NANO thruster significantly contributes to the overall success of our mission. Moreover, the thruster's low power consumption Table XXII feature is yet another valuable asset. By minimizing energy consumption, we can ensure optimal

energy utilization and guarantee that ample power resources remain available for other critical subsystems onboard our satellite [17]. Efficient power management allows us to allocate resources to different mission operations and payloads, ultimately enhancing the overall efficiency and productivity of our satellite mission. The ENPULSION NANO thruster stands out as the ideal choice to fulfill our mission objectives, owing to its combination of compact size, utilization of FEEP technology, precision, and low power consumption. Through its deployment, we are confident in our ability to achieve mission success, optimize satellite performance, and accomplish our objectives with heightened efficiency and reliability.

TABLE XXII
THRUSTER PARAMETER

Parameter	Value
Specific Impulse Range (s)	2000 to 6000
Dynamic Thrust Range (µN)	10 to 350
Mass (Dry /Wet)(g)	680 / 900
Power (W)	8 to 40
Propellant Mass (g)	220 ± 5 %

E. Station Keeping- Anibal & Danica

The technique of maintaining a satellite's orbital location within prescribed limitations throughout time is known as station keeping. A 6U satellite's competence to keep its desired position and orbit in space depends on station keeping. It ensures that the satellite remains in its operational region and performs its intended functions effectively. Without station keeping, the satellite's orbit would deteriorate due to numerous triggers, including atmospheric drag and gravitational disturbances, forcing it to drift away from its target area. Periodic corrections are required to compensate for orbital disturbances produced by factors such as gravitational forces and air drag. The satellite may overcome these forces and maintain its position by conducting station-keeping movements. This enables it to fulfil mission objectives like communication, Earth observation, or scientific data collecting with precision and reliability.

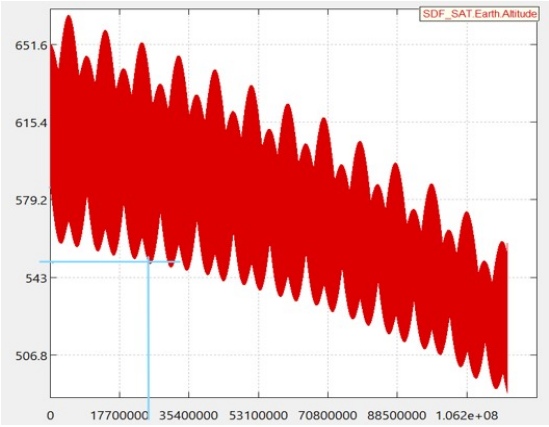

Fig. 9. Station Keeping

In this study, we utilized the GMAT (General Mission Analysis Tool) Simulation to analyze and optimize station-keeping maneuvers for a satellite operating at an orbital altitude of 585 km. The simulation specifically focused on assessing the effects of a recurring 30 km orbit degradation, which takes place at an altitude of 555 km every 292 days. Figure 9 represents the station-keeping regime.
Through rigorous analysis, we determined the precise time required for the satellite to execute a maneuver, denoted as *tmaneuvers*, which was calculated to be approximately 1.3406E5 seconds. This duration corresponds to 4.58 days, signifying the range within which station-keeping adjustments must be made to ensure the satellite's stable and desired orbital position.

F. De-Orbiting - Anna

De-orbiting can be done by using propellant to decrease the altitude or in a passive way by using the atmospheric drag of the earth, which is present in LEO. To increase the possible mission duration and decrease the necessary mass for de-orbiting, we decided to use the second option with atmospheric drag. This increases the possible mission duration with respect to the battery lifetime and power generation since no power is required for the drag sail during de-orbiting. The simulation is done with the tool STELA by CNES and uses the drag area computed with random tumbling, the NRLMSISE-00 atmosphere model, the solar radiation pressures corresponding to the year 2033 (launch in 2028 and mission duration of 5 years), and the influence of sun and moon perturbations as input. The random tumbling calculation is conservative but valid for our case because we assume that during de-orbiting no power for attitude control will be available and the satellite will start tumbling due to environmental perturbations. In a first approximation, the idea was to use the drag sail ADEO-N from HPS GmbH with a sail area of 2 m^2, the mass of 1kg, and a volume of 1U [47]. In many iterations, the solar array area was increased to such a high value, that the arrays themself act as drag sail and ensure to meet the requirement of a de-orbit within 5 Years, which is already requested by SpaceX when choosing one of their rockets for a ride share [48] according to the new FCC regulations [49]. The de-orbit calculation using the Software STELA from CNES shows in Figure 10, that the satellite is de-orbited within 3.78 years.

XIV. SATELLITE STRUCTURE - RAKESH

The satellite structure should hold all the subsystems while ensuring that these subsystems carry out their function effectively. The following considerations were made for different subsystems:

- Observation Payload
  - The camera should point towards the nadir.
  - The camera's lens should be kept cold and away from heat sources.
- Attitude Determination and Control System (ADCS)
  - The ADCS should be kept close to the satellite's principle axes to increase the actuators' effectiveness.

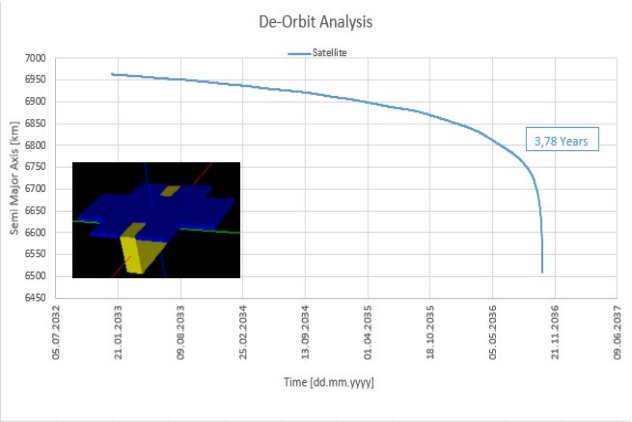

Fig. 10. De-Orbit Analysis of the satellite

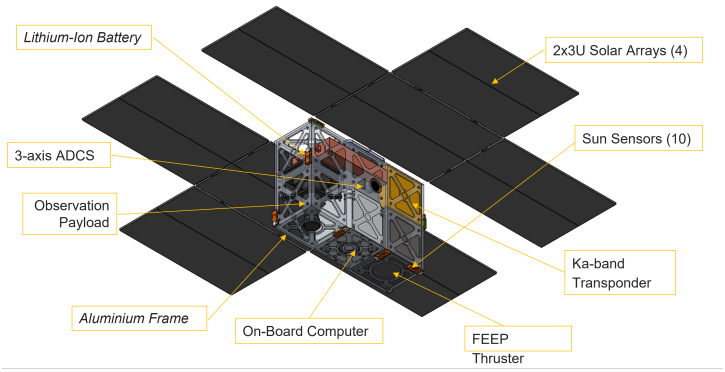

Fig. 11. Structural Configuration of the satellite

- The star sensor and horizon sensor should be pointing outward.
- The sun sensor should be on the peripheral of the satellite and uncovered during the deployment phase to help with attitude determination for detumbling.

- Thermal and Power Systems
  - The battery generates heat; hence, it should be kept away from the camera's lens and close to other electronic subsystems to keep them at ambient operating temperature.
  - The solar driver should be able to keep the solar arrays close perpendicular to the sun.
- Propulsion System
  - The propulsion system should point in the opposite direction of the flight direction.
  - The structure should fit in a standard orbital deployer.
- Tracking, Telemetry, and Control (TT&C) System
  - The antennas should point up, as the Telesat Lightspeed™ satellite constellation is in higher orbit.
- Onboard Computer
  - The onboard computer should be kept from the ADCS system to avoid electrical and magnetic interference.

After reviewing the above considerations, the 6U CubeSat structure is used, which is deployable from Poly-Picosatellite Orbit Deployer (P-Pod). The satellite's frame will be made of aerospace-grade **Aluminium Alloy AA6061** due to its higher strength-to-weight ratio, higher manufacturability, ease of anodizing, and availability for all temper conditions [50].

Figure 11 represents the final structural configuration of the satellite.

XV. Conclusions and Future Directions - All

This report represents the preliminary design of the satellite for monitoring plastic waste in the Pacific Ocean. The satellite would be a 6U CubeSat which is deployable from P-PODs. The integrated solution is used for payload, ADCS, TT&C and propulsion, which makes them suitable for fitting in the standard CubeSat structures. This also eliminates the issues with the compatibility of various components functioning together. The wide 4x2 6U gimbaled solar arrays and the single-cell battery system powers the entire spacecraft. The selection of the ground station, along with the launcher and launch site, is done in terms of achieving suitable performance and lower costs.

Further work needs to be done concerning the development of Onboard Computer (OBC) and Onboard Computer Software (OBSW). An equipment interconnection network has to be determined to relay information between OBC and other subsystems. A specific OBSW needs to be developed, which accounts for various flight phases and different modes of operations. The software also needs to account for failure detection and isolation of the system. In the case of payload and TT&C data exchange, encoding and decoding protocols need to be set up in accordance with Consultative Committee for Space Data Systems (CCSDS).

This report serves as a guideline for further detailed design.

References

[1] Willey J. Larson and James R. Wertz. *Space Mission Analysis and Design*. 3. ed. Microcosm Press, 1999. ISBN: 1-881883-10-8.

[2] berlin-space-tech. *HRVI-6HD 2ND GENERATION*. 2023. URL: https://www.berlin-space-tech.com/portfolio/hrvi-6hd-2nd-gen/ (visited on 06/05/2023).

[3] simera-sense. *The xScape100 Key Parameters*. 2023. URL: https://simera-sense.com/products/xscape100-2/ (visited on 06/05/2023).

[4] esa. *About WorldView-2*. 2023. URL: https://earth.esa.int/eogateway/missions/worldview-2 (visited on 06/03/2023).

[5] J. Vos E. Grobbelaar. *xScape50 - Interface Control Document*. June 28, 2022.

[6] satcatalog. *JG-P1100G Push-Broom Camera*. 2023. URL: https://www.satcatalog.com/component/jg-p1100g-push-broom-camera/ (visited on 06/05/2023).

[7] simera-sense. *HyperScape50 Product Specifications*. 2023. URL: https://simera-sense.com/products/xscape50/hyperscape50/ (visited on 06/05/2023).

[8] Ulrich Walter. *Astronautics*. 3. ed. Springer, 2008.

[9] esa. *Types of orbits*. 2020. URL: https://www.esa.int/Enabling_Support/Space_Transportation/Types_of_orbits (visited on 05/03/2023).

[10] DA Vallado. "Kepler's equation and kepler's problem". In: *Fundamentals of Astrodynamics and Applications, 3rd ed.; Springer: New York, NY, USA* (2007), pp. 49–136.

[11] Sung Wook Paek. "Reconfigurable satellite constellations for geo-spatially adaptive Earth observation missions". PhD thesis. Massachusetts Institute of Technology, 2012.

[12] Sung Wook Paek et al. "Sun-synchronous repeat ground tracks and other useful orbits for future space missions". In: *The Aeronautical Journal* 124.1276 (2020), pp. 917–939.

[13] "ReliaSat KKa-TRSP-1929 Satellite Transponder Module 17-21 and 27-31 GHz Product Datasheet". In: *ReliaSat KKa-TRSP-1929 Datasheet* (). URL: https://reliasat.com/wp-content/uploads/2023/03/KKa-TRSP-1929-1.pdf.

[14] CubeSpace. *Interface Control Document*. 2022. URL: https://www.cubespace.co.za/products/gen-1/integrated-adcs/cubeadcs/ (visited on 07/25/2023).

[15] M. Pasaretti and R. Hayes. "Development of a Solar Array Drive Mechanism for CubeSat: Developed by: Honeybee Robotics Spacecraft Mechanisms Corporation in cooperation with MMA Design". In: NASA/CP-2010-216272 (2010).

[16] GOMSpace. *gs-ds-nanopower-p80-100_(DS_-_1047423_-_1_-_10)_-_1*. 2023. URL: https://gomspace.com/shop/subsystems/power/nanopower-p80.aspx (visited on 07/24/2023).

[17] Enpulsion. *Enpulsion Datasheet*. 2018. URL: https://www.enpulsion.com/order/enpulsion-nano/ (visited on 07/25/2023).

[18] NASA. "2022 State of the Art Small Spacecraft Technology Report". In: NASA/TP-2022-0018058 (2023).

[19] Saft. *VES_16_battery_data_sheet*. 2023. URL: https://www.saft.com/media-resources/knowledge-hub?text=&market=331&doctype=&sort=newest&submit=Search (visited on 07/24/2023).

[20] Eaglepicher. *LP33081 30 Ah Space Cell 0123*. 2023. URL: https://www.eaglepicher.com/products/secondary-batteries-rechargeable/ (visited on 07/24/2023).

[21] Eaglepicher. *LP 33450 43Ah Space Cell 0319*. 2023. URL: https://www.eaglepicher.com/products/secondary-batteries-rechargeable/ (visited on 07/24/2023).

[22] EAS. *UHP341440 NCA data sheet*. 2023. URL: https://eas-batteries.com/markets/space (visited on 07/24/2023).

[23] EAS. *HE602030 NCA Data sheet*. 2023. URL: https://eas-batteries.com/markets/space (visited on 07/24/2023).

[24] GOMSpace. *gs-ds-nanopower-bp4 (DS - 1013024 - 1 - 3.0) - 1*. 2023. URL: https://gomspace.com/shop/subsystems/power/nanopower-bp4.aspx (visited on 07/24/2023).

[25] M. R. Concha. *Life-Cycle Testing of Mars Surveyor Program Lander Lithium-Ion Battery*. 2006. URL: https://web.archive.org/web/20130909212150/http://www.grc.nasa.gov/WWW/RT/2005/RP/RPC-reid.html (visited on 07/24/2023).

[26] ISISPACE. *Small satellite _ CubeSat Solar Panels - ISISPACE*. URL: https://www.isispace.nl/product/isis-cubesat-solar-panels/ (visited on 07/24/2023).

[27] Sparkwing. *Sparkwing_DataSheet_20230127*. 2023. URL: https://sparkwing.space/satellite-solar-panels/ (visited on 07/24/2023).

[28] SpaceTech GmbH. *STI-DS-03-20229-191_Datasheet_SolarArrays_2022-9-28_final_web*. 2023. URL: https://spacetech-i.com/solar-arrays (visited on 07/24/2023).

[29] Endurosat. *6U Single Deployable Solar Array Datasheet*. 2023. URL: https://endurosat.com/cubesat-store/all-cubesat-modules/6u-solar-panel/ (visited on 08/09/2021).

[30] MMA Design. *MMA Design Products Solar Arrays*. URL: https://mmadesignllc.com/products/solar-arrays/ (visited on 07/24/2023).

[31] M. M. Finckenor. "Multilayer Insulation Material Guidlines". In: NASA/TP-1999-209263 (1999).

[32] Ernst Messerschmidt and Stefanos Fasoulas. *Raumfahrtsysteme*. 5th ed. Springer, 2017. ISBN: 978-3-662-49637-4. DOI: https://doi.org/10.1007/978-3-662-49638-1.

[33] Lisa Jonsson. *Simulations of Satellite Attitude Maneuvers - Detumbling and Pointing*. 2019.

[34] Stark J. Fortescue P. Swinerd .G. *Spacecraft Systems Engineering*. 4th ed. WILEY, 2011. ISBN: 978-0-470-75012-4.

[35] Newton A et al. "Investigation Reaction Wheel Configuration and Control Law Pairings for CubeSats in the Presence of Faults". In: *CSME Congress* (2020).

[36] California Polytechnic State University. "6U CubeSat Design Specification". In: *NASA explorer* (2016).

[37] SpaceX. *SmallSat Rideshare Program*. 2023. URL: https://www.spacex.com/rideshare/ (visited on 07/27/2023).

[38] SpaceX. *Falcon User's Guide*. 2021. URL: https://www.spacex.com/media/falcon-users-guide-2021-09.pdf (visited on 07/27/2023).

[39] Wikipedia contributors. *Falcon 9 — Wikipedia, The Free Encyclopedia*. https://en.wikipedia.org/w/index.php?title=Falcon_9&oldid=1164778186. [Online; accessed 25-July-2023]. 2023.

[40] Wikipedia. *Vandenberg Space Force Base — Wikipedia, the free encyclopedia*. [Online; as of July 28, 2023]. 2023. URL: %5Curl%7B%20https://de.wikipedia.org/w/index.php?title=Vandenberg_Space_Force_Base&oldid=234242572%20%7D.

[41] Exolaunch. *Exolaunch introduces Eco Space Tug Program*. 2021. URL: https://exolaunch.com/news_54 (visited on 07/26/2023).

[42] exolaunch. *Exolaunch Heritage Missions*. 2023. URL: https://exolaunch.com/heritage (visited on 07/14/2023).

[43] "Telesat Lightspeed™ - Transmission Security (TRANSEC)". In: *Telesat Lightspeed™ Whitepaper* (). https://www.telesat.com/wp-content/uploads/2022/05/Telesat-Lightspeed-Transmission-Security-White-Paper-Telesat.pdf.

[44] Federal Communications Commission (FCC). *The Establishment of Policies and Service Rules for the Non-Geostationary Satellite Orbit, Fixed Satellite Service in the Ka-Band*. 2003. URL: https://docs.fcc.gov/public/attachments/FCC-03-137A1.pdf.

[45] Federal Communications Commission (FCC). *SPECIFIC INSTRUCTIONS FOR SCHEDULE S*. 2016. URL: https://enterpriseefiling.fcc.gov/schedules//resources/Instructions%20for%20Schedule%20S%20vApr2016.pdf.

[46] German Aerospace Center (DLR). *Ground Station Weilheim*. URL: https://www.dlr.de/rb/PortalData/38/Resources/dokumente/leistungen/DLR_RB_Portfolio_GroundStationWeilheim.pdf (visited on 07/22/2023).

[47] HPS GmbH. *ADEO-on angel wings*. 2023. URL: https://www.hps-gmbh.com/portfolio/adeo-on-angel-wings/ (visited on 07/24/2023).

[48] SpaceX. *Rideshare Payload User's Guide*. 2022.

[49] FCC. *FCC Open Meeting Agenda September 2022*. 2022.

[50] Afaf M. Abd El-Hameed and Y. A. Abdel-Aziz. "Aluminium Alloys in Space Applications: A Short Report". In: *Journal of Advanced Research in Applied Sciences and Engineering Technology* (2021).

[51] "ThinKom Solutions and Telesat Sign Agreement to Integrate Ka-Band Antennas on Telesat Lightspeed™ Satellite Network". In: *Telesat Press Release* (). https://www.telesat.com/press/press-releases/thinkom-solutions-and-telesat-sign-agreement-to-integrate-ka-band-antennas-on-telesat-lightspeed-satellite-network/.

[52] "ThinAir® Ka2517 Technical Specifications". In: *ThinAir® Ka2517 Datasheet* (). https://www.thinkom.com/wp-content/uploads/2018/09/ka2517-datasheet_9_18_web.pdf.

[53] SpaceX. *SpaceX HQ Gallery*. 2017. URL: https://twistedsifter.com/2017/01/spacex-launch-landing-jan-2017-hq-gallery/ (visited on 07/20/2023).

[54] Rocket and Space Technology. *MSISE-90 Model of Earth's Upper Atmosphere*. 1996. URL: http://www.braeunig.us/space/atmos.htm (visited on 07/23/2023).

[55] CSABA JÉGER. *Determination and compensation of magnetic dipole moment in application for a scientific nanosatellite mission*. 2017.

[56] National Aeronautics and Space Administration [NASA]. "Spacecraft Magnetic Torques". In: *NASA* (1969).

XVI. Appendix

A. Appendix A: MATLAB Functions - Anibal

This appendix points out the inputs and main objectives involved in each function developed using MATLAB.

1) Orbit, Payload & Requirement Functions: This category involves functions that perform orbital determination, payload selection, and setting requirements.

- *requirements.m*
  - Input: Ground Sampling Distance (GSD) and mission duration (t_mission)
  - Purpose: This function calculates the specific requirements for the mission based on the desired Ground Sampling Distance and the total mission duration. The obtained requirements serve as the foundation for subsequent calculations.
- *satellite_sizing.m*
  - Input: Satellite dimensions (mass, volume, etc.).
  - Purpose: This function determines the optimal sizing of the satellite based on the provided dimensions. It takes into account the mass, volume, and requirements of the spacecraft.
- *camera.m*
  - Input: Design parameters of the camera.
  - Purpose: This function calculates the characteristics of the camera that will be integrated into the spacecraft. It considers factors such as resolution, field of view, and data collection capabilities.
- *orbit.m*
  - Input: Parameters from camera.m and spacecraft requirements.
  - Purpose: The *orbit.m* function calculates the characteristics of the Solar Synchronous Orbit (SSO) specific to the camera's characteristics and the spacecraft requirements.
- *deOrbitDeltaV*
  - Input: Parameters from *satellite_sizing.m* and spacecraft characteristics.
  - Purpose: The *orbit.m* function calculates the characteristics of the Solar Synchronous Orbit (SSO) specific to the camera's characteristics and the spacecraft requirements.

2) Power & Thermal Subsystem Functions - Anibal+Anna: This category involves functions that calculate battery capacity requirements, temperatures attained throughout the spacecraft, battery and solar array sizing, power requirements, and temperature checks for every subsystem.

- *power_budget.m*
  - Input: Total power determination of the spacecraft. Uses power budget from all other subsystems.
  - Purpose: The function calculates the total power required for the spacecraft to support all its subsystems. It considers power consumption during different operational modes and ensures sufficient power supply.
- *battery_sizing.m*
  - Input: Eclipseduration from *orbit.m*, total power requirements and DoD.
  - Purpose: The function determines the required battery capacity to meet the spacecraft's power demands during eclipses and total power consumption. It ensures adequate energy storage for uninterrupted operation.
- *array_sizing.m*
  - Input: Solar array requirements of the satellite with values obtained from power requirements *power_budget.m* and array degradation.
  - Purpose: The function calculates the required solar array size to generate the necessary power for the spacecraft's operations. It ensures a reliable and sustainable power supply under solar exposure.
- *thermal_design.m*
  - Input: Used power in eclipse and sun-phase from *power_budget.m*, Sun flux, Earth Albedo and Earth radiation.
  - Purpose: The function performs a thermal analysis under hot and cold environmental conditions to get the equilibrium temperatures.
- *thermal_check.m*
  - Input: Equilibrium temperatures from *thermal_design.m* and operational temperature range of the subsystems.
  - Purpose: The function checks if the spacecraft's components are operating within their specified survival and operational specified temperature ranges. Therefore, it ensures that components remain within their operational limits.

3) ADCS Subsystem Functions - Anibal+Falk: This category involves functions that perform orbital determination, payload selection, and setting requirements.

- *torque_magnetic.m*

  - Input: Parameters from *satellite_sizing.m* and Earth's magnetic field characteristics.
  - Purpose: Calculate the torque generated by the magnetic field acting on the spacecraft.
- *torque_aero.m*
  - Input: Parameters from *satellite_sizing.m* and atmospheric modelling.
  - Purpose: Calculate the torque generated through aerodynamic forces experimented by the spacecraft in LEO.
- *torque_slew.m*
  - Input: Parameters from *satellite_sizing.m* and maximum moment of inertia.
  - Purpose: Calculate the slew torque of the spacecraft generated with the biggest moment of inertia.
- *torque_gravity.m*
  - Input: Parameters from *satellite_sizing.m* and Earth characteristics.
  - Purpose: Calculate the torque generated through gravitational potential difference in the spacecraft.
- *torque_solar.m*
  - Input: Parameters from *satellite_sizing.m* and solar parameters.
  - Purpose: Calculate the torque generated through solar radiation pressure.
- *detumble_torque.m*
  - Input: Parameters from *satellite_sizing.m* and detumbling requirements.
  - Purpose: Calculate the torque required to detumble the spacecraft.
- *momentum_storage_eq.m*
  - Input: Torques from all other torque-calculating functions and parameters from *satellite_sizing.m*.
  - Purpose: The function calculates the reaction wheel's required momentum to be stored to compensate for the torques.

4) Additional Functions: This category involves functions that perform orbital determination, payload selection, and setting requirements.

- *polynomialsolver.m*
  - Purpose: This function attempts to aid the *orbit.m* function in its orbit determination, by solving through integration, the orbital elements. However, due to the specific nature of the mission, this function was not implemented in the final analysis.
- *function_template.m*
  - Purpose: This script serves as a template for creating new functions if additional calculations or analyses are required during the spacecraft design process.

B. Appendix B: Propulsion System Trade-Off Analysis - Anibal

Appendix B includes all the trade-off analyses performed for the propulsion system architecture selection and the requirements considered in the process.

TABLE XXIII
TRADE-OFF ANALYSIS 1. PROPELLANT SYSTEMS' TECHNICAL DATA

Sub Criteria	Isp [s]	Thrust [N]	T mission	Re-ignitability	System complexity	Total Mass & Volume	Required Power	Sys. Compatibility	Contamination	Technology Status	Availability	Total Cost
Hybrid	250	800	Low	Low	Mid	High	Mid-Low	Mid	Mid	Not flight proved	Mid-Low	Mid
Liquid Monopropellant	225	600	Low	Mid-High	Mid-Low	High	Mid-Low	Mid	High	Fully developed	High	High
Liquid Bipropellant	340	1000	Low	Mid-High	High	High	Mid-Low	Mid	High	Fully developed	High	Mid-High
Electrostatic	10000	0.5	High	High	Mid-High	Low	High	Low	Mid-Low	Fully developed	High	Low
Electromagnetic	5000	200	Mid	High	High	Low	High	Low	Low	In Development	Low	Low
Nuclear (Solid Core)	1000	+1000	Mid-Low	Low	Mid-High	Mid	Mid	Low	High	Not Flight Proved	Low	Mid-Low
Other (Solar Sail)	-	1	High	Mid-Low	Low	Mid-Low	None	Mid-High	None	Flight proved	Low	Low

TABLE XXIV
TRADE-OFF ANALYSIS 2. PARAMETER RELEVANCE FOR THE MISSION

	Isp [m/s²]	Thrust [N]	T mission	Re-ignitability	System complexity	Total Mass & Volume	Required Power	Sys. Compatibility	Contamination	Technology Status	Availability	Total Cost	Sum
Isp [m/s²]	X	2	1	1	1	3	2	2	2	3	1	3	44
Thrust [N]	2	X	1	1	1	3	2	2	2	3	1	3	44
T mission	3	3	X	2	1	3	3	2	1	2	3	2	42
Re-ignitability	3	3	2	X	3	3	3	2	2	2	1	3	45
System complexity	3	3	1	2	X	3	2	2	2	3	2	3	43
Total Mass & Volume	1	1	1	1	1	X	1	1	1	1	1	3	44
Required Power	2	2	1	1	2	3	X	1	1	3	1	3	44
Sys. Compatibility	2	2	2	2	2	3	3	X	2	2	1	3	44
Contamination	2	2	3	2	2	3	3	2	X	2	2	3	44
Technology Status	1	1	2	2	1	3	1	2	2	X	2	2	44
Availability	3	3	1	3	2	3	3	3	2	2	X	2	44
Total Cost	1	1	2	1	1	1	1	1	1	2	2	X	44
Sum	23	23	17	18	17	31	24	20	18	25	17	30	263
Weight	0.087	0.087	0.065	0.068	0.065	0.118	0.091	0.076	0.068	0.095	0.065	0.114	1

TABLE XXV
TRADE-OFF ANALYSIS 3. PARAMETER CRITERIA

ECSS Criteria	**Performance**		**Mision req.**		**Resulting Layout**			**Compatibility and contamination**		**Experience**	**Availability of components**	
Score Assigned	Isp [s]	Thrust [N]	T mission	Re-ignitability	System complexity	Total Mass & Volume	Required Power	Sys. Compatibility	Contamination	Technology Status	Availability	Total Cost
1	0-225	0-1	High	Low	High	High	High	Low	High	Haven't Started	Low	High
2	225-299	1-250	Mid-High	Med-High	Mid-High	Mid-High	Mid-High	Mid-Low	Mid-High	In Development	Mid-Low	Mid-High
3	300-999	250-500	Mid	Med-High	Mid	Mid	Mid	Mid	Mid	Not Flight Proved	Mid	Mid
4	1000-4999	500-7500	Mid-Low	High	Mid-Low	Mid-Low	Low-Mid	Mid-High	Mid-Low	Flight Proved	Mid-High	Mid-Low
5	5000+	750-1000+	Low	High	Low	Low	Low	High	Low	Fully Developed	High	Low

TABLE XXVI
TRADE-OFF ANALYSIS 4. CRITERIA ASSIGNMENT TO EACH PROPULSION SYSTEM

	Isp [m/s²]	**Thrust [N]**	**T mission**	**Prop. Re-start**	**System complexity**	**Total Mass & Volume**	**Required Power**	**Sys. Compatibility**	**Contamination**	**Technology Status**	**Availability**	**Total Cost**
Hybrid	2	5	5	1	3	2	4	3	3	3	2	3
Liquid Monopropellant	1	4	5	4	4	1	4	3	1	5	5	1
Liquid Bipropellant	3	5	5	4	1	2	4	3	1	5	5	2
Electrostatic	5	1	1	5	2	5	1	1	4	5	5	5
Electromagnetic	5	2	3	5	1	5	1	1	5	2	1	5
Nuclear	3	5	4	1	2	3	2	1	1	3	1	4
Other(Solar Sail)	2.5	1	1	2	5	4	5	1	5	4	1	5
Weight	0.080	0.080	0.110	0.064	0.061	0.106	0.083	0.076	0.068	0.102	0.057	0.114

TABLE XXVII
TRADE-OFF ANALYSIS 5. SCORE CALCULATION

	Isp [m/s²]	**Thrust [N]**	**T mission**	**Prop. Re-start**	**System complexity**	**Total Mass & Volume**	**Required Power**	**Sys. Compatibility**	**Contamination**	**Technology Status**	**Availability**	**Total Cost**	**SCORE**
Hybrid	0.174904943	0.437262357	0.323193916	0.068441065	0.19391635	0.235741445	0.365019011	0.228136882	0.205323194	0.285171103	0.129277567	0.342205323	2.99
Liquid Monopropellant	0.087452471	0.349809886	0.323193916	0.273764259	0.258555133	0.117870722	0.365019011	0.228136882	0.068441065	0.475285171	0.323193916	0.114068441	2.98
Liquid Bipropellant	0.262357414	0.437262357	0.323193916	0.273764259	0.064638783	0.235741445	0.365019011	0.228136882	0.068441065	0.475285171	0.323193916	0.228136882	3.29
Electrostatic	0.437262357	0.087452471	0.064638783	0.342205323	0.129277567	0.589353612	0.091254753	0.076045627	0.273764259	0.475285171	0.323193916	0.570342205	3.46
Electromagnetic	0.437262357	0.174904943	0.19391635	0.342205323	0.064638783	0.589353612	0.091254753	0.076045627	0.342205323	0.190114068	0.064638783	0.570342205	3.14
Nuclear	0.262357414	0.437262357	0.258555133	0.068441065	0.129277567	0.353612167	0.182509506	0.076045627	0.068441065	0.285171103	0.064638783	0.456273764	2.64
Other(Solar Sail)	0.218631179	0.087452471	0.064638783	0.136882129	0.323193916	0.47148289	0.456273764	0.076045627	0.342205323	0.380228137	0.064638783	0.570342205	3.19

C. Appendix C: Mission Requirements - All

In Appendix C, all mission requirements have been included. These correspond to operational, functional, and mission constraints. Additionally, all subsystem requirements are also included.

TABLE XXVIII: Mission Requirements

Category	**ID**	**Keywords**	**Description**
Functional	1-000		
Functional	1-001	Accuracy, Camera	The mission shall have a ground sampling distance of at least 36m.
Functional	1-002	Accuracy	The mission shall geolocate the data with an accuracy of 0.1°
Functional	1-003	Orbit	The ground track shall repeat itself after a maximum of 10 days.
Functional	1-004	Orbit, Camera	The camera shall cover at least 90% of the Pacific Ocean.
Operational	2-000		
Operational	2-001	Orbit	The satellite shall be in an orbit around the earth with a LEO altitude.
Operational	2-002	Operation Time	The mission shall operate for at least 5 years.
Operational	2-003	Groundstation	The data shall be transmitted to the Groundstation once a day.
Operational	2-004	Orbit	The final orbit shall have an inclination larger than 66,56°.
Operational	2-005	Environment	The satellite shall survive the orbital environment.
Operational	2-006	Linkbudget	The mission shall support a maximum of 10 simultaneous users.
Operational	2-007	Orbit,De-Orbit	The satellite shall de-orbit within 5 years at "end-of-life".
Operational	2-008	Launch,Launcher	The launcher shall be able to bring the satellite in an orbit 100 km away from its target orbit.
Operational	2-009	Launch,Launcher	The spacecrafts volume shall comply with the launchers user manual requirements
Operational	2-010	Launch,Launcher	The spacecrafts mass shall comply with the launchers user manual requirements
Constraints	3-000		
Constraints	3-001	Environment,Temperature	The satellite shall withstand temperatures -60 up to 100 degrees.
Constraints	3-002	General	The mission shall consist of 1 satellite.
Constraints	3-003	General	The mission shall launch in 2028.

Constraints	3-004	Orbit	The target orbit shall have an eccentricity below 0.1.
Subsystems	4-000		
Camera	4-101	Accuracy,Camera	The images shall be taken with a wavelength of λ = 880nm.
Camera	4-102	Accuracy,Camera	The images shall be taken with a wavelength of λ = 443nm.
TT&C	4-201	Linkbudget,Antenna	The losses of the antenna shall not exceed 3dB.
Solar Arrays	4-301	Power	The solar arrays shall provide at least 117W for power.
Solar Arrays	4-302	Power,Size	The solar arrays shall have a size of at least 0.3 $\hat{m2}$.
Solar Arrays	4-303	Power	The solar arrays shall be rotatable and always being perpendicular to the Sun.
Battery	4-401	Power	The battery shall have enough capacity to provide the Power during eclipse.
Battery	4-402	Power	The battery shall survive at least 27 000 life cycles.
Battery	4-403	Power	The battery shall be Li-Ion.
Propulsion	4-501	Delta-V	The propulsion system shall provide the required DV to reach the target orbit.
Propulsion	4-502	Delta-V	The propulsion system shall provide sufficient DV to keep the target orbit.
Propulsion	4-503	Size	The propulsion system shall have a volume smaller than 1 $\hat{m3}$.
Propulsion	4-504	Station keeping	The operational orbit shall not deviate more than 30 km from the target orbit.
Propulsion	4-505	Station keeping	The propulsion system shall perform the station-keeping maneuvers.
ADCS	4-601	Maneuverability	The pointing range about the x/y/z axis shall be 0 to 360 degrees.
ADCS	4-602	Detumbling	The ADCS shall be able to detumble the satellite from 5.7 [°/s].
ADCS	4-603	Pointing	The pointing accuracy shall be at least 0.1°.
ADCS	4-604	Slew	The ADCS shall be able to rotate the satellite at an angular velocity of at least 0.25 [°/s].
ADCS	4-605	Desaturating	The ADCS shall be able to desaturate the stored momentum within one orbit].

D. Appendix D: Detailed Link Budget - Rakesh

TABLE XXIX: Link Budget

Link Parameters	**Value**	**Units**	**Initial Notes**
Uplink Frequency	**27**	**GHz**	**Telesat to the CubeSat**
Uplink Function	**Command**		
Telesat Antenna Type	**Flat Antenna [51]**		
Antenna Dimensions	1.4224 x 0.8128	m	Datasheet [52]
Antenna Area	1.16	m^2	Datasheet [52]
Antenna Efficiency	55.00%	%	Typical value (Assumed)
Gain	48.12	dBi	Formula
EIRP, Gateway	48.5	dBW	Datasheet [52]
Propagation Range	500	km	
Space Loss	-175.06	dB	Formula
Atmospheric Losses	0	dB	No atmospheric losses above 20km altitude
Net Path Loss	-175.06	dB	
Satellite Antenna, Type	**Flat Antenna [13]**		

Antenna Efficiency	70.00%	%	Assumed
Gain	20	dBi	Datasheet [13]
Line Loss on Satellite	-2	dB	Typical value selected for this scenario (Assumed)
Received Carrier Power Per User, C	-108.56	dBW	
Receiver Noise Antenna Temperature	700	K	At 1000km altitude
Effective Temperature of feed	314	K	Highest Temperature during Sun
Reference Temperature	290	K	
Reciever Noise Figure	2.5	dB	Datasheet [13]
Line Power Ratio	0.75		Rx Output Power / Rx Input Power
Effective System Noise Temperature, Ts	658.17	K	At 1000km altitude
System Noise Temperature	-28.2	dB-K	Typical value selected for this scenario (Assumed)
G/T	48.18	dB/K	
Receiver C/N_o	91.86	dB-Hz	
Single User Data Rate	44	Mbps	Input from Datasheet
Data rate per user	76.43	dB-Hz	
Available E_b/N_o, Uplink	**15.43**	**dB**	
Downlink Frequency	**17.8**	**GHz**	
Downlink Function	**Telemetry & Data**		
Satellite Antenna, Type	**Flat Antenna [13]**		
Antenna Efficiency	70.00%	%	Assumed
Antenna Gain	20	dBi	Datasheet [13]
Backoff and Line Loss	-4.5	dB	Assumed
Satllite Tx Power	27	dBm	Datasheet [13]
EIRP per Line Loss	42.5	dBW	Satllite Tx Power
Propagation Range	500	km	
Space Loss	-171.44	dB	
Atmospheric Losses	0	dB	Typical value selected for this scenario
Net Path Loss	-171.44	dB	
Telesat Antenna Type	**Flat Antenna [51]**		
Antenna Dimensions	1.4224 x 0.8128	m^2	Datasheet [52]
Antenna Area	1.16	m^2	Datasheet [52]
Antenna Efficiency	55.00%	%	Assumed
Gain, G	44.5	dBi	Formula
Line Loss	-2	dB	Assumed
Receive Carrier Power Per User, C	-86.44	dBW	
System Noise Temperature	-28.2	dB-K	Typical value selected for this scenario
G/T	72.68	dB/K	
Receiver C/N_o	170.34	dBW	
Data Rate per user	76.43	dB-Hz	
Available E_b/N_o, Downlink	**93.91**	**dB-Hz**	
End-to-End E_b/N_o	**15.43**	**dB**	**Uplink plus Downlink**
Modem Implementation Loss	-1.2	dB	Representative for this scenario
Required E_b/N_o	**5.41**	**dB**	**[1], Table 16-12**
Link Margin	**8.8**	**dB**	
Single User Data Rate	44	Mbps	
Code Rate, ρ	5/6		For 8-PSK, [1] Table 16-12

Single User Bandwidth	35.376	MHz	
BER	4.52E-08		For 8-PSK, [1] Fig 16-16
Pixels	4086	px	Payload Datasheet
No. of Lines	128		
Error Bits	1.89E-01		
Error Pixels	2.36E-02		

E. Appendix E : Launcher and Orbital Transfer Vehicle - Ditsa

Appendix E includes visual representation of the launch vehicle and decided upon orbital transfer vehicle depictions. The following Figure 12 is that of our decided launch vehicle Falcon 9 in correspondece with the SmallSat Rideshare Program. Figure 13 shows the way Exolaunch, the OTV will help in launching and deploying our satelite to the designated orbit as per our mission. Also the Figures 14 and 15 depict the 2 different types of configurations with regards to the satellite deployment, namely the **Standard Configuration** and the **Pro Configuration** respectively.

Fig. 12. SpaceX's Falcon 9 Launcher [53]

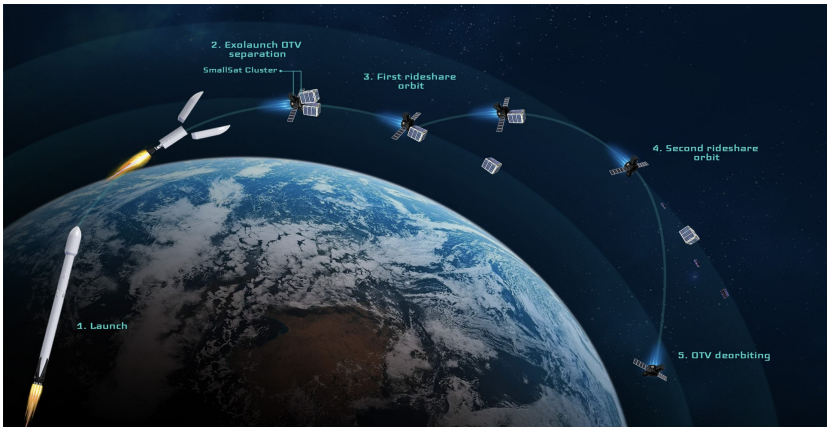

Fig. 13. Exolaunch [41]

Fig. 14. Standard Configuration [41]

Fig. 15. Pro Configuration [41]

The Standard configuration is best used for moving satellites to a customised orbit altitude after they've been deployed from a launch vehicle on a set rideshare orbit. The Pro configuration is best suited with a hybrid propulsion system, which combines the advantages of green propulsion and the unique capabilities of electric propulsion system as well. [41]

F. Appendix F: ADCS - Environmental Disturbances - Falk

1) Aerodynamic Drag: As the satellite operates in low Earth orbit, it is still subjected to atmospheric drag from the outer layers Earth's atmosphere. This aerodynamic drag torque can be computed by:

$$T_a = \frac{1}{2}\rho C_d A_r V^2 (cp_a - cm) \tag{27}$$

T_a is the aerodynamic drag torque, ρ is the atmospheric density of a given altitude, A_r is the reference surface, C_d the spacecraft's drag coefficient, V is the orbital velocity, cp_a and cm are the centres of the aerodynamic pressure and mass respectively. For the calculations, a constant value of $\rho = 7.55E-12\frac{kg}{m^3}$ is used, representing the worst-case scenario at an altitude of $580km$ under extremely high solar activity[54]. The drag coefficient was set to $C_d = 2.2$[34] and the misalignment of the centre of mass and aerodynamic centre of drag was assumed to be $0.05m$, both based on reference values[1] as to calculate those aerodynamic parameters would require further analysis. For the exposed reference surface area A_r is taken as the maximum surface area of the satellite's body. More accurate values could be obtained using a raster-based method as described in[55].

2) Gravity Gradient: Due to misalignment of the satellite's centre of mass with its the centre of gravity, torques are generated. The torques can be calculated by the simplified formula[1]:

$$T_g = \frac{3\mu}{2R^3}(I_{zz} - I_{yy})\sin 2\theta \tag{28}$$

T_g is the generated torque about the X principal axis, $\mu = 0.3986 * 10^{15}\frac{m^3}{s^2}$ is the Earth's gravitational constant, R is the radius. I the moment of inertia of the satellite which is obtained from the satellite's CAD model. ϕ and θ are the roll and pitch angles respectively.

3) Solar radiation pressure: The phenomenon that sunlight carries momentum results in a momentum exchange when the sunlight is reflected at a surface, thereby generating a torque. This torque depends on various factors like surface material reflectiveness and the angle of the satellite relative to the sun. During this early design phase, to accurately predict the solar ration pressure is challenging due the satellite's diverse components. For initial estimations, a uniform reflectance is assumed and the solar radiation torque computed by:

$$T_s = \frac{\Phi}{c}A_s(1+q)(cp_s - cm)\cos\varphi \tag{29}$$

T_s is the solar radiation torque, Φ is the solar constant and $c = 3 * 10^8\frac{m}{s}$ is the speed of light. A_s is the sunlit surface area, q is the reflectance factor, φ is the angle of incidence of the Sun, cp_s and cm are the centers of solar radiation pressure and mass respectively. For the calculations the reflectance factor was set to $q = 0.6$ and the difference between the centres of mass and solar radiation pressure to $cps - cm = 0.1$ based on reference values[1] as in this design phase they are not known

precisely. φ is set to $\varphi = 0°$, as being perpendicular represent the worst-case scenario. Earth's radiation disturbance torques are neglected as they are relatively small compared to the solar radiation pressure.

4) Magnetic Torque: Nearly every Spacecraft possesses a residual magnetic moment that interacts with Earth's magnetic field, thus generating a magnetic torque. Modelling the Earth's magnetic field as a dipole, the maximum possible magnetic torque can be calculated by[1]:

$$T_m = DB = D(\frac{M}{r^3}\lambda) \tag{30}$$

T_m is the magnetic torque, D describes the spacecraft's residual dipole moment and B the magnetic field strength. The magnetic constant $M = 7.8 * 10^{15} Tm^3$ and r is radius. λ is a function of the magnetic latitude. For the calculations, λ is set to $\lambda = 1.9$ due to the high inclined orbit. The residual dipole moment is set to $D = 0.1 Am^2$ based on an per unit estimation for non-spinning spacecrafts[56].

G. Appendix G: Parameter Relevance for the Propulsion System Architecture Trade-Off Analysis - Anibal

This appendix carefully evaluates each parameter's significance to ensure that the chosen propulsion system aligns with the mission's specific requirements and constraints. These parameters have been ranked in order of importance. Additionally, these relevance scores are reflected in the grading system included in Table XXIV.

The *total mass and volume* of the propulsion system directly affects the physical constraints of the spacecraft. To be contained in a 1U, it is crucial to optimize the system, ensuring efficient integration and functionality without compromising overall mission payload capacity.

The *cost* impacts the project's budget and financial feasibility. Therefore, keeping the cost within acceptable limits is essential to ensure that the mission remains financially viable within the allocated resources.

The *technology status* parameter evaluates the maturity and reliability of each architecture. A well-established, flight-proven technology would reduce the risks associated with the development and implementation, increasing the overall mission's success probability.

The *required power* influences the total power demand required by the architecture and will be a great component in determining the size and capacity of the batteries and solar arrays. Thus, ensuring the efficient use of power resources is crucial for supporting other critical spacecraft systems and maximizing the mission's operational capabilities.

The *specific impulse* and *thrust*, both being performance parameters, are determined to be equally relevant as they directly affect the propulsion system's efficiency and performance. Higher *Isp* values indicate better propellant efficiency, while higher *thrust* values contribute to faster orbital maneuvers, crucial for meeting mission objectives and orbital adjustments such as station keeping.

The chosen architecture must be compatible with the other spacecraft systems. Therefore, the *system's compatibility* reduces the risk of technical issues and facilitates a smoother functioning of the mission.

Contamination and *re-ignitability* are equally relevant. On one hand, the contamination parameter assesses the potential risks of pollution. Ensuring low contamination is an ever-growing concern within the space industry and its push for greener propulsion systems. On the other hand, the system shall be re-ignitable, capable to perform multiple firings and orbital adjustments. This ability proves critical to achieving the desired orbit and maintaining station-keeping requirements throughout the mission.

The propulsion system must be *available*. Ensuring readily available components simplifies the procurement process and reduces potential delays in the mission timeline.

Lastly, the *system's complexity* assesses the overall complexity of the architecture. Minimizing the complexity reduces development risks and enhances overall reliability and ease of operation.